AD-A115 534 AIR FORCE INST OF TECH WRIGHT-PATTERSON AFB OH SCHOO--ETC F/G 9/1
LASER INDUCED FLUORESCENCE OF BARIUM EVAPORATING FROM A DISPENS--ETC(U)
MAR 82 S M ZEMYAN

UNCLASSIFIED AFIT/GNE/PH/82M-13 NL

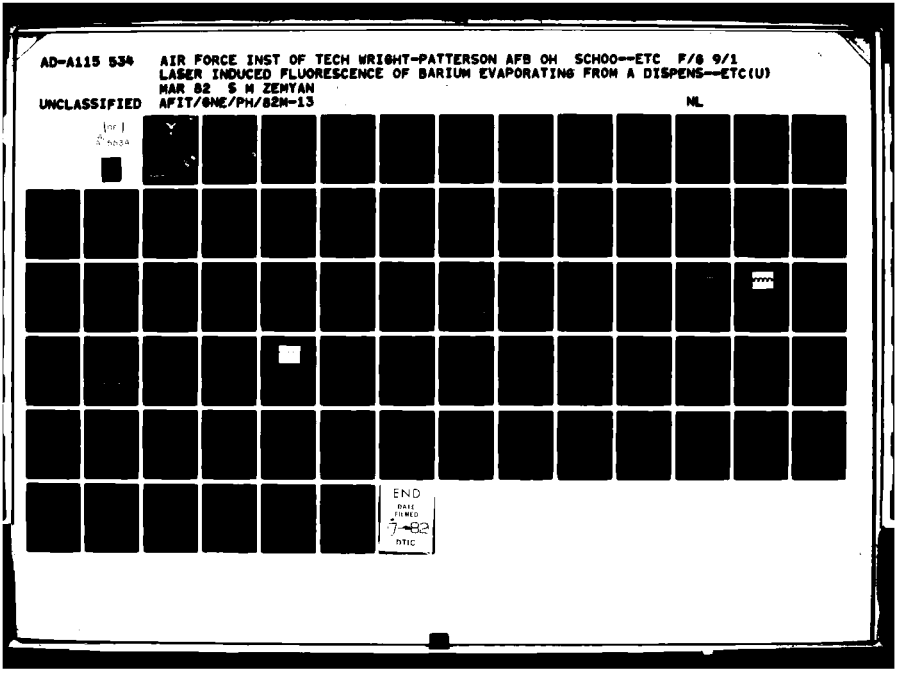

UNITED STATES AIR FORCE

AIR UNIVERSITY

AIR FORCE INSTITUTE OF TECHNOLOGY

Wright-Patterson Air Force Base, Ohio

LASER INDUCED FLUORESCENCE OF BARIUM EVAPORATING FROM A DISPENSER CATHODE

THESIS

AFIT/GNE/PH/82M-13 Stephen M. Zemyan
2nd Lt USAF

Approved for public release; distribution unlimited

AFIT/GNE/PH/82M-13

LASER INDUCED FLUORESCENCE OF BARIUM EVAPORATING FROM A DISPENSER CATHODE

THESIS

Presented to the Faculty of the School of Engineering
of the Air Force Institute of Technology
Air University
in Partial Fulfillment of the
Requirements for the Degree of
Master of Science

by
Stephen M. Zemyan
2nd Lt USAF
Graduate Nuclear Engineering
March 1982

Approved for public release; distribution unlimited

Acknowledgements

I particularly want to thank my advisors for this project, Dr. Theodore Luke and Dr. Won Roh. Their guidance and insight, in approaching both theoretical and experimental problems, helped me on many occasions.

I want to thank Mr. James Miskimen, whose frequent assistance with operating and modifying equipment saved me much time and taught me many facts.

I also want to thank Dr. Perry Yaney and the University of Dayton for lending me the laser that was crucial to my experiment.

This thesis effort has been one of the best of my educational experiences. It has taught me methods of formulating, researching and solving a detailed problem.

Contents

List of Figures

Table

Abstract

A continuous wave dye laser is used to induce resonance fluorescence in Ba atoms evaporating from a thermionic dispenser cathode. The laser is tuned to the 553.5nm Ba I line by making use of the optogalvanic effect in a hollow cathode discharge tube. Photon counting equipment is used to measure the Ba fluorescent intensity as a function of cathode temperature and laser power. Ba concentrations and evaporation rates as functions of temperature are derived from the fluorescent intensity.

Laser induced fluorescence is established as a technique for examining various species evaporating from cathodes. The technique can be used in attempts to determine cathode failure mechanisms.

I Introduction

General Comments

With the development of solid state electronics, many requirements for vacuum tubes have disappeared. However, several applications, including communication satellites, still exist and foster research in tube technology. Travelling wave tubes (TWT's), used as transmitters in satellites, must be designed for long operational lifetimes. One of the principal life limiting components of a TWT is its thermionic cathode, the failure mechanisms of which are not well known.

Research into cathode degradation can proceed along at least three different lines. First, attempts could be made to understand the chemistry taking place within the cathode that produces species that form the active electron emitting layer. Second, research could be done to find the nature of the emitting layer - its formation, make up, and eventual disruption. Finally, studies could be made of the vapors boiling from the cathode so that operating mechanisms could be inferred. This research effort focuses on the third area by using laser induced resonance fluorescence to identify species in the vapor and to measure their concentrations.

Fluorescence spectroscopy has been used to measure minute concentrations of atoms and molecules in flames, discharges, and vapors. Atoms in the vapor absorb laser radiation at the frequency of an electronic, rotational, or vibrational transition. Then the absorbed energy is re-

radiated in directions that
agation of the exciting ase
tion is detected using photo
fluorescent intensity can th
density of the fluorescing e

Problem Statement

The purpose of this inv
method for determining evapo
from thermionic cathodes. S
ating element in cathodes, t
Ba detection. By finding th
on various operational paran
anisms may be better unders

Order of Presentation

This report begins with
ionic cathodes. It describe
ation and presents some of
ance. The purpose is to pro
the problem of cathode failu
ground on laser induced fluo

Next is a section on ho
plied to the study of Ba.
relates the Ba number densi
intensity.

Then come sections tha
cedures used in this invest
sions, and recommendations

radiated in directions that may be different from the propagation of the exciting laser beam. The fluorescent radiation is detected using photon counting techniques. Detected fluorescent intensity can then be related to the number density of the fluorescing atoms.

Problem Statement

The purpose of this investigation is to establish a method for determining evaporation rates of various species from thermionic cathodes. Since Ba is an important activating element in cathodes, the method is to be applied to Ba detection. By finding the dependency of Ba evaporation on various operational parameters, cathode operating mechanisms may be better understood.

Order of Presentation

This report begins with a background section on thermionic cathodes. It describes some of the theories of operation and presents some of the features of cathode performance. The purpose is to provide a general understanding of the problem of cathode failure. This is followed by background on laser induced fluorescence.

Next is a section on how fluorescence detection is applied to the study of Ba. An equation is developed that relates the Ba number density to the detected fluorescent intensity.

Then come sections that describe the equipment and procedures used in this investigation, and the results, conclusions, and recommendations for further research.

II Background

Cathodes

The purpose of this section is to review the construction and operation of thermionic cathodes. Thermionic emission is discussed and then various designs for cathodes are presented. Studies of cathode chemistry and surface phenomena have led to contradictory models of the formation and the behavior of the emitting surface. These models are reviewed and used to understand possible cathode failure mechanisms.

Cathodes in vacuum tubes supply current by thermionic emission. Thermionic emission is best understood by looking at a diagram of the distribution of electron energies in a metal. (See figure 1.) At absolute zero, no electrons escape to vacuum because none have energies above the Fermi level. To be emitted, an electron must have an energy of $(E_F + \phi)eV$, where ϕ is the work function and E_F is the Fermi energy. At high temperatures, the Fermi-Dirac distribution changes so that some electrons have an energy greater than the potential of the surface, and can therefore escape.

The number of electrons with enough energy to be emitted is dependent on the work function and the temperature. The Richardson-Dushman equation describes this relation.

$$J = 120T^2 \exp(-\phi/kT) \qquad (1)$$

where

J is the emitted current density in A/cm^2,

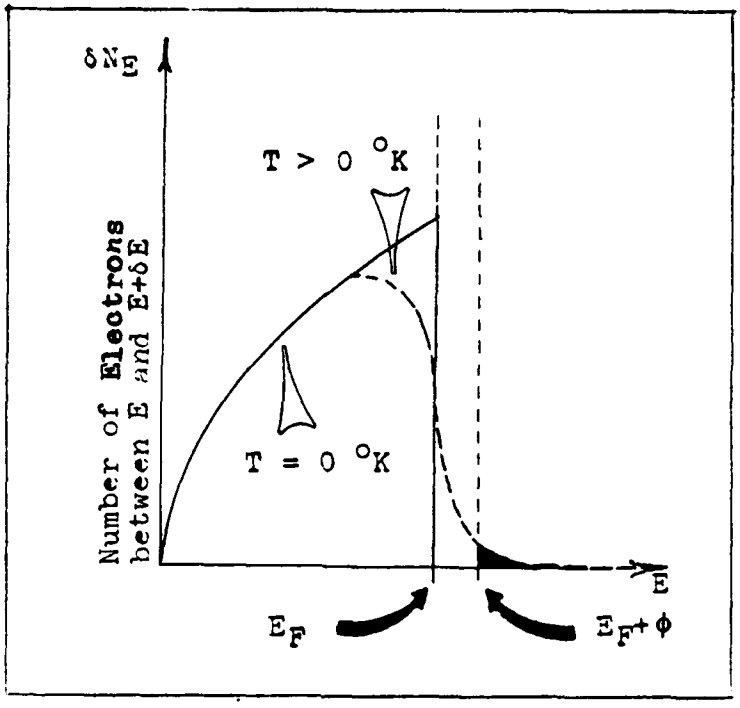

Figure 1. Distribution of Electron Energies in a Metal (Ref 1:163)

T is the temperature in K,
k is the Boltzmann constant, and
ϕ is the work function at T in eV.

For a given current density, the higher the work function, the higher the operating temperature must be. Therefore, great effort is expended to find surfaces with low work functions. As an example, to have 1 A/cm^2 of emission from clean W, with ϕ = 4.54eV, T must be 2575K. However, if ϕ = 2.0eV, T need only be 1220K. This example is chosen because a cathode surface is often made of W contaminated in such a way that its work function is approximately 2.0eV (Ref 2 :262).

One way to lower the work function of a metal is to cover the surface with a thin layer of electropositive atoms.

These atoms assemble in a dipole layer with the positive side above the surface. This positive region accelerates electrons perpendicularly away from the surface and thereby lowers the work function (Ref 3:535). If the surface layer is electronegative, the work function is similarly increased. Coverage by a negative film is called poisoning of the cathode (Ref 4:354). Much of the study of cathodes has to do with the formation and behavior of these layers that effect the work function.

The two predominant kinds of thermionic cathodes are the oxide film cathode and the dispenser cathode. The first operates at low current densities, below 0.2 A/cm^2, while the latter may work above 4 A/cm^2 (Refs 5:397; 6).

The oxide film cathode consists of a layer of barium/strontium oxides (BaO, SrO) deposited on a base that is usually Ni. The oxide film is greater than 50μm thick. A heater in the cathode induces reactions which reduce some of the oxides. An outermost layer forms which lowers the work function. This layer may contain both Ba and BaO, but its exact composition is unknown. Heat causes evaporation of the film components. Failure of the cathode probably occurs when the film has been depleted of activating components to the extent that an effective electropositive layer no longer exists (Refs 4:357-358; 5:397). Since no mechanism exists for replenishing the oxide layer, cathode lifetimes are limited by the small amount of activating material in the layer.

The dispenser cathode was developed in the late 1940's

in response to a need for cathodes of higher current density and longer lifetime. The "L cathode" was developed first. It consisted of an open Mo chamber capped with a porous W plug. The chamber contained a tablet of $(Ba\text{-}Sr)CO_3$. When heated, CO_2 was driven off, leaving BaO and SrO which then diffused through the porous W cap to the emitting surface (Refs 7:177; 8:156-157). In 1953, the "impregnated cathode" was developed and soon replaced the L type. (See figure 2 for drawings of the L and impregnated cathodes.) The imregnated cathode consisted of a porous W plug saturated with Ba and Ca aluminates (Al_2O_3) and mounted on a Mo body containing a heater (Ref 9:233). During activation, the aluminates are reduced leaving Ba and Ca tungstates (Ba_3WO_6 for example) in the W pores while Ba, Ca, and their oxides migrate through the plug. Ba and O bond with W at the surface to form an emitting layer; however, the nature of the Ba-O-W bond is not known. Depletion of Ba by evaporation is thought to limit the cathode life. However, since much more Ba can be included in the dispenser cathode than in the oxide film cathode, the dispenser type can be run at higher current densities for longer times (Ref 4:358).

The remainder of this section is a review of the activation chemistry and surface phenomena of the impregnated dispenser cathode.

The impregnant in the impregnated cathodes consists of varying amounts of BaO, CaO, and Al_2O_3. Actually, free BaO and CaO do not exist in the mixture. Instead, compounds

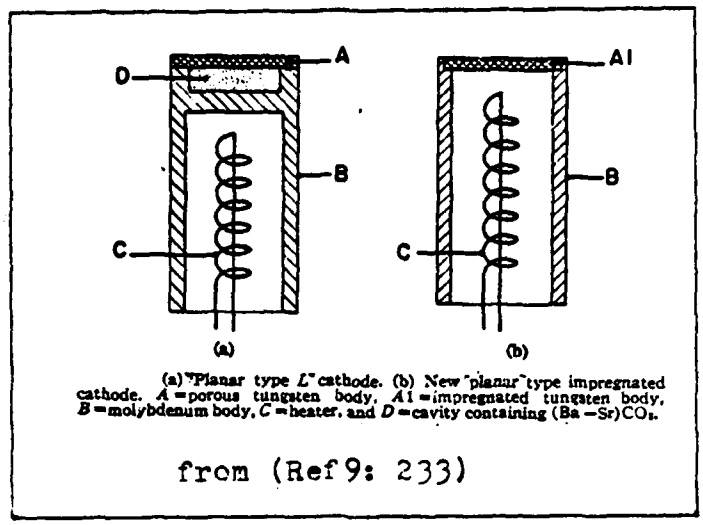

(a) "Planar type L" cathode. (b) New "planar" type impregnated cathode. A = porous tungsten body, Al = impregnated tungsten body, B = molybdenum body, C = heater, and D = cavity containing $(Ba-Sr)CO_3$.

from (Ref 9: 233)

Figure 2. Cross Sectional Views of "L Type" and "Impregnated Dispenser" Cathodes

such as $Ba_3Al_2O_6$, $BaAl_2O_4$, $Ba_2CaAl_2O_6$, $BaCa_2Al_2O_6$, $Ca_3Al_2O_6$, and $CaAl_2O_4$ are found. The mixture is prepared by reacting BaO and CaO with Al_2O_3 to form the above compounds. The proportions of the reactants are chosen to yield a final mixture with as a low a melting point as possible. If the cathode contained free BaO or CaO, they would react with water vapor and CO_2. To minimize this contamination, the Ba and Ca are bonded in alkaline aluminum oxides which are unreactive until heated (Refs 7:180; 10:1470-1471).

When the impregnated W cathode is heated, a number of possible reactions can take place, some leading to the production of free Ba. Although all sources agree that Ba is produced in the cathode, no agreement exists on the chemistry taking place. The compounds of Al_2O_4 do not react as easily with W as those of Al_2O_6. Therefore, if $BaAl_2O_4$, or $CaAl_2O_4$ is formed, it is considered to be lost from the Ba production

cycle (Ref 7:130). However, the Al_2O_6 compounds may be reduced by reactions of the following type.

$$Ba_3Al_2O_6 \leftrightarrow 2BaO + BaAl_2O_4 \quad (2)$$

$$\text{then } 6BaO + W \leftrightarrow Ba_3WO_6 + 3Ba \quad (3)$$

$$\text{or } 4BaO + W \leftrightarrow BaWO_4 + 3Ba \quad \text{(Ref 9:1470).} \quad (4)$$

Since the WO_4 and the WO_6 compounds are stable, the Ba in those compounds cannot be freed. The amount of Ba produced by these reactions depends on whether Ba_3WO_6 or $BaWO_4$ is more likely to form.

A complete chemical description must take the behavoir of the Ca products into account. $Ca_3Al_2O_6$ can be reduced by reactions similar to those for $Ba_3Al_2O_6$. Additionally, the reduction of the 2-1 and 1-2 compounds $Ba_2CaAl_2O_6$ and $BaCa_2Al_2O_6$ must be accounted for (Ref 11:2898-2899). For example,

$$Ca_2BaAl_2O_6 \leftrightarrow BaAl_2O_4 + 2CaO$$

$$\text{or } CaAl_2O_4 + BaO + CaO \; . \quad (5)$$

The number of possible reactions taking place is quite large. Although the processes are not completely understood, Some general statements can be made.

1) Since the tungstates are stable compounds, they will tend to accumulate at the reaction sites instead of being reduced further.

2) Also, the $-Al_2O_4$ compounds will accumulate since they are less reactive than the Al_2O_6 compounds.

3) Free Ba and Ca will be produced in amounts depending on the original mixture and the extent to which reduction is completed.

4) BaO and CaO will also be produced. These molecules are able to migrate from the reaction sites and may reach the surface in appreciable quantities. They may further be reduced, freeing Ba and Ca.

The free species reaching the emitting surface affect the emission properties of the cathode. As mentioned previously, an electropositive layer on a metal surface tends to lower the work function. For the impregnated cathode, this layer is provided by Ba and O on or near the W surface. Models of the exact composition of this layer vary,but all reports agree that both Ba and O are found at the cathode surface. When this layer is in some way disrupted, the work function rises and the current density drops. Cathode failure is often defined as occurring when the current density drops below a certain operational level. An understanding of cathode surface phenomena is needed to understand the failure mechanisms.

Forman points out that at least five models of the cathode surface have been proposed (Ref 2:259).

1) A monolayer of BaO and Ba on W.

2) A monolayer of CaO activated by Ba.

3) A BaO layer several atoms thick.

4) A Ba monolayer or less on slightly oxidized W.

5) A monolayer or less of Ba and O on W.

Some of these seem to be quite similar. In fact, the greatest dispute is over the nature of bonding between Ba, O, and W. From the results of Auger electron spectroscopy, Forman concludes that O is not tightly bound to either Ba or W. He further concludes that only a partial monolayer of Ba and O may exist over much of the cathode life (Ref 2:273).

Rittner claims that the surface is a monolayer of O covered by a full monolayer of Ba for the entire cathode life (Ref 12: 4344). Brodie and Jenkins believe that the surface contains O and free Ba, with CaO at the pore ends only (Ref 13: 29). Even though no widely accepted theory exists explaining the cathode surface, several general statements can be made.

1) Ba and O exist on the surface in a thin layer.

2) The O is not tightly bound to the Ba.

3) This layer is important in lowering the surface work function, allowing high emission.

Much useful information on cathode performance has come from the study of the evaporation rates of various species and may be linked to the cathode lifetime.

Ba, for example, evaporates at a rate that decreases with the square root of time (Ref 14:159). Also, Ba concentration is lowered in the cathode to a depth which increases with the square root of time (Ref 11:2398). As Ba is removed from the pores near the surface, the Ba reservoir doesn't rise to fill them. Therefore, as time increases, free Ba must migrate further to reach the surface. Because the Ba meets a greater impedance with time in its migration,

the evaporation rate may be expected to drop with time (Ref 15: 5278).

As a comparison, Ca is removed at a rate decreasing with the cube root of time (Ref 11:2898). This difference from the removal rate of Ba is not understood. CaO is used in cathodes because its addition to the impregnating mixture increases the electron emission (Ref 7:183). However, the mechanism by which CaO affects the emission is not understood.

The variation of current density during the cathode lifetime is reported to be different by various researchers. Forman finds that the current drops steadily until the cathode ceases operation (Ref 16:1546). Rittner believes that the current is constant until a catastrophic failure occurs (Ref 12:4345). Forman's explanation is that during operation, the supply rate of Ba to the surface decreases causing coverage by less than a monolayer of Ba. As this partial layer becomes patchier, the emission current drops until it reaches the failure level. Rittner's explanation is that the supply rate of Ba is high enough throughout the life to maintain a complete monolayer of coverage; therefore, the emission is constant. When the supply of Ba is exhausted, the cathode fails.

Both experiments link the decrease in current density to depletion of Ba from the impregnant. In fact, several failure mechanisms have been proposed (Ref 2:268-270).

1) Depletion of Ba from the reservoir.

2) Increased impedance to Ba flow through the W pores due to the accumulation of reaction products.

3) Increased impedance due to W crystallization at high temperatures.

4) Loss of O from the surface.

This last mechanism is in another area that requires investigation. The method of transport of O to the surface is not well understood. It could come in the form of BaO or it could be present in the W plug as a result of the manufacturing process. The O would then need to diffuse to the surface (Ref 2:270). The rate of O loss from the surface is not known. Some suspect it is small compared to the Ba evaporation rate while others believe it to be larger (Refs 2: 269; 17:3297-3298). Of course, if BaO is evaporated in large quantities, O would be lost. Therefore it would be of interest to know the evaporation rates of both Ba and BaO.

The information presented in this summary has been collected using a wide range of experimental techniques. X-ray diffraction and the electron microprobe were used to measure Ba and Ca removal as a function of the cathode depth. Surface analysis came from Auger electron spectroscopy, the scanning electron microscope, and electron emission microscopy. Work function and emission measurements were made by placing an electron collection anode near the cathode. Some evaporation measurements were made using mass spectroscopy (Ref 11:2894). The work done in this project adds another method of measuring evaporation rates to the list.

The above techniques have been used to learn much about cathode operation. However, several fundamental problems must be solved to gain further insight into cathode failure.

1) Determine the role of Ca in increasing emission.

2) Learn what reactions take place to produce free Ba and Ca.

3) Determine the nature of the emitting surface.

4) Discover what species are evaporated, and at what rates.

5) Learn why Ba and Ca depletion rates change as they do with time.

6) Determine whether emission does actually vary with time before failure.

Laser Induced Resonance Fluorescence

Resonance fluorescence is a two step interaction between photons and bound electrons. First, an atom (or molecule) absorbs a photon at the frequency of an electronic, rotational, or vibrational transition, leaving the atom in an excited state. After an interval which is the lifetime of the excited state, a photon is spontaneously emitted, leaving the atom in a lower energy state. If the initial and final states are the same, then the absorbed and emitted photons must be of the same frequency. The fluorescence is then said to be resonant with the exciting radiation.

In this experiment, a tunable dye laser is used to provide the stimulating radiation. It provides a high spectral intensity of light and can be tuned to the proper frequency to induce resonance fluorescence. The intensity of

the fluorescence can be related to the number of fluorescing atoms. Therefore, by measuring the fluorescent intensity, the atomic concentration can be found. Because of the narrow linewidth of the laser, fluorescence can be induced in a single species of a multi-component sample. In fact, this technique allows highly selective measurement of small atomic or even isotopic concentrations (less than 100 atoms/cm^3).

Resonance fluorescence has been used to identify atoms in discharges, flames, and vapors from furnaces. Since it is particularly applicable to free atoms, fluorescence could be used to examine the constituents of a vapor from a cathode. Concentrations and evaporation rates could be found of Ba, BaO, Ca, CaO, and other species.

The next chapter will describe how laser induced resonance fluorescence is applied specifically to Ba detection. For a more general treatment of resonance fluorescence, the reader should consult the following sources (Refs 18, 19, and 20).

III Application of Laser Induced Resonance Fluorescence to Ba

In this chapter it is shown how resonance fluorescence can be used to measure Ba concentrations. The energy levels of Ba are studied. The geometry of the experiment is discussed to show how the laser beam interacts with the Ba produced by the cathode, and how the detection optics intercept the fluorescent photons. Using this information, a relation is developed between the measured fluorescent intensity and the Ba number density. This relation is used to analyze the experimental data in chapter V.

The transition in Ba from which fluorescence is detected is the $6s6p\ ^1P_1 - 6s^2\ ^1S_0$ 553.5nm transition. (See the energy level diagram of Ba in figure 3.) A laser beam of known intensity is passed above and parallel to the cathode surface. Atoms evaporating from the cathode (including Ba) pass through the laser beam and are induced to fluoresce. The intensity of the fluorescence from the Ba atoms is measured with photon counting equipment. By knowing how Ba responds to the laser light, the fluorescence intensity may be related to the Ba concentration.

The response of Ba to laser stimulation may be understood by modeling the atom as a three energy level system. The exciting radiation is resonant with the 3-1 transition. The upper level is also transitionally coupled to level 2, which is metastable. Since the metastable state decays only

to the ground state, a three level model is appropriate.

Values for the lifetimes of these states are known or can be approximated. The lifetime of the 6s6p $^1P_1$ level (3) for decay to levels 1 and 2 is 8.20ns (Ref 21:A376). This state decays to two other states with a branching ratio of 99% to $^1S_0$ and 1% to $^1D_2$ (Ref 22:418). Other sources quote this ratio at 96%, but 99% is the result of a more recent experiment (Ref 23:237). The branching ratio implies that $\tau_{31} \cdot 100 = \tau_{32}$, where the τ's are the lifetimes for decays between particular levels. From the relation

$$1/\tau_3 = 1/\tau_{31} + 1/\tau_{32} , \quad \tau_3 = 8.2\text{ns} \tag{6}$$

we find

$$\tau_{31} \cong \tau_3 = 8.2\text{ns} \tag{7}$$

$$\tau_{32} \cong 100\tau_3 = 820\text{ns} \tag{8}$$

The remaining transition is from the metastable $^1D_2$ to the ground state. The lifetime is not known, but has been estimated to be greater than 1ms (Ref 24:269). Going one step further, the lifetime of the metastable can be considered infinite for this experiment because the lifetime is greater than the time an atom will spend in the laser beam. The speed of a Ba atom travelling through the beam can be estimated to be $v_z = \sqrt{kT/m}$, where k is Boltzmann's constant, T is the temperature (of the cathode, 1225K), and m is the mass of the atom. This is the root mean square speed in one direction of an atom in a Maxwellian distrib-

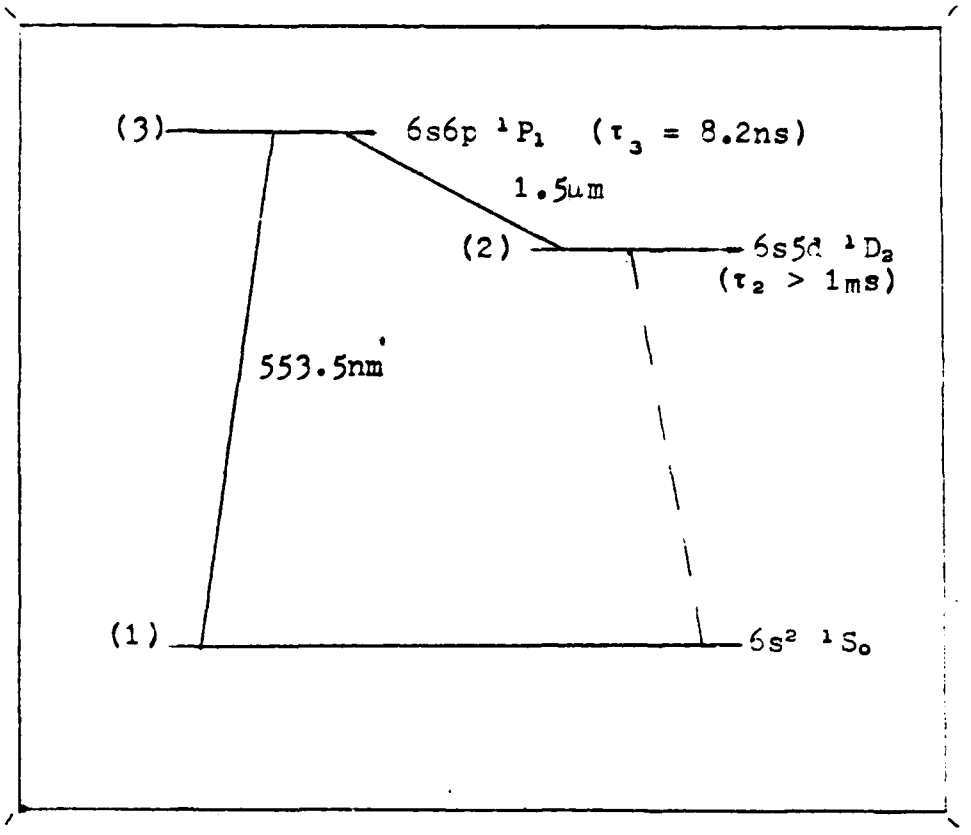

Figure 3. Partial Energy Level Diagram of Barium I

ution at temperature T. Although the Ba atoms probably aren't in a Maxwellian distribution, this does give an estimate of the speed of 280m/s perpendicular to the laser beam. A more accurate estimate of the velocity would need to account for the energy bonding the atoms to the surface and the distribution of directions with which the atoms leave the surface. Since the beam is approximately 0.5mm wide above the cathode, the atoms spend about 1.8μs in the beam, or only 0.2% of the lifetime of the metastable state. Therefore, the conclusion can be drawn that once an atom is pumped into the metastable state, it will no longer be able

to contribute fluorescent photons.

If all Ba atoms that enter the beam leave in the metastable state, then the fluorescent intensity can easily be related to the Ba number density. The condition that all atoms be pumped into the metastable state will be addressed later. Since the branching ratio of the upper level to the ground state is taken to be BR = 99%, an atom will have to radiate spontaneously $BR/(1-BR) = 99$ times, on average, before it is pumped into the metastable state. Therefore, the maximum number of photons radiated spontaneously by each atom is on the average 99. Note that if BR = 96%, as has been previously reported, the number of photons per atom is 24. If BR is slightly higher, say 99.5%, then the number of photons is 199. Since BR is close to unity, a small error in its value would be significant. All subsequent results are based on BR =99%.

To find the intensity of the fluorescence, the number of atoms being excited per second must be determined. The number of atoms passing through the fluorescing volume per second is $N_t Av$, where N_t is the Ba density, v is the rms speed, and A is an estimate of the horizontal cross section of the fluorescing volume. For this analysis, N_t is assumed to be constant across the fluorescing volume. The volume is the cylindrical volume of the laser beam directly above the cathode. (See figure 4.) The number of photons radiated per second is $99N_tAv$ and the fluorescent power is $h\nu 99N_tAv$ in J/s, where ν is the photon frequency in Hz. However, all of these photons are not registered by the det-

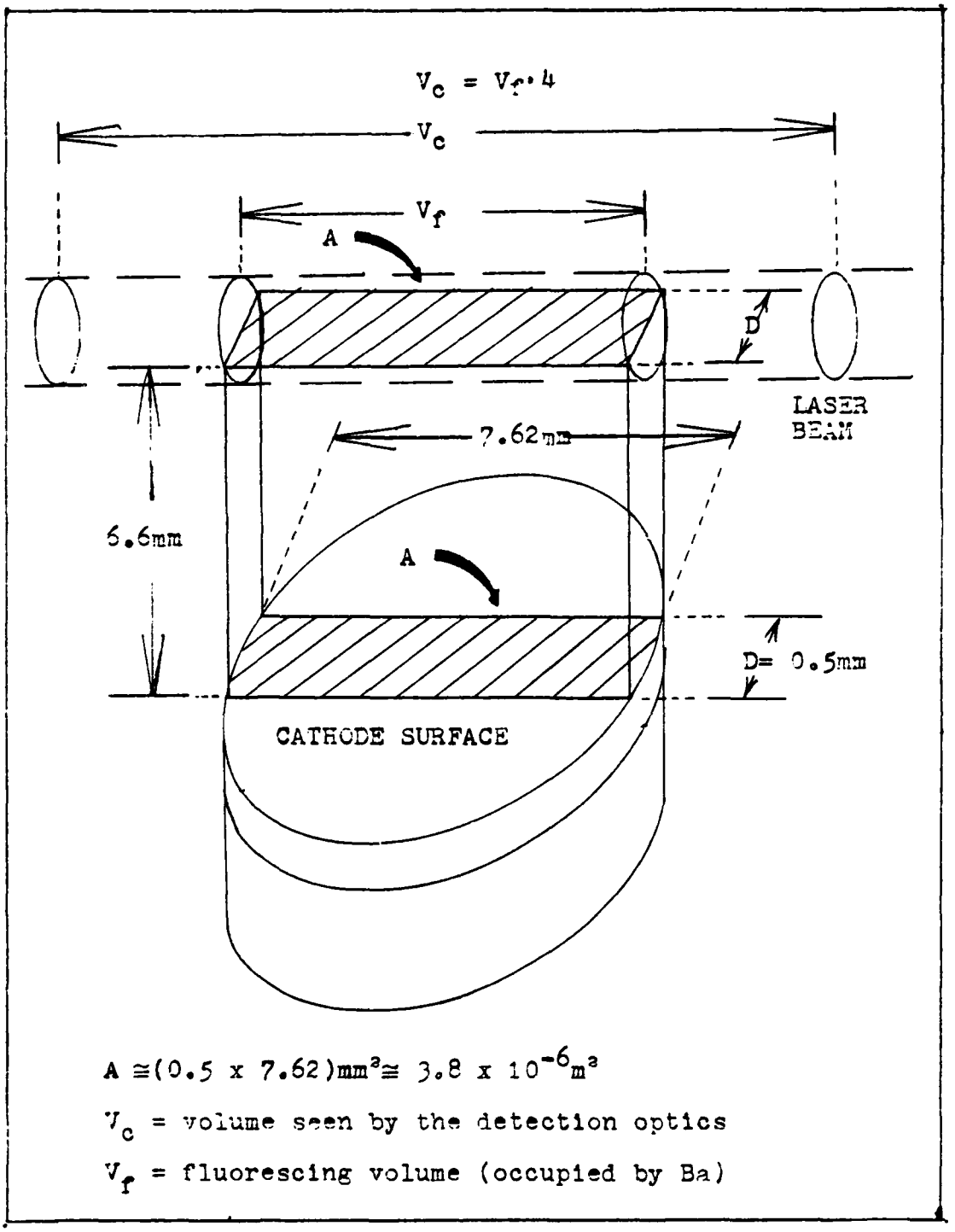

Figure 4. Drawing of V_f and V_c

ection system due to collection losses and inefficiencies. The detected fluorescent power will be

$$P_f = 99 h\nu N_t v \frac{\Omega}{4\pi} \epsilon A \qquad (9)$$

where

Ω is the solid angle subtended by the detection optics, and
ϵ accounts for the efficiency of the photomultiplier and the losses due to optical components.

Using the method described by Benham, $\Omega V_c \epsilon$ can be found by an independent calibration (Ref 25:8-10). For a review of this method, see appendix B. V_c is the volume of the laser beam seen by the detector. However, the fluorescing volume shown in figure 4 is smaller than V_c by a factor of 4. V_f is the volume of the beam containing Ba atoms and is taken to be the volume of the beam directly over the cathode. Note that

$$V_f \approx (D/2)^2 \cdot \pi (A/D) = (AD\pi)/2, \qquad (10)$$

where

D is the beam diameter.

Therefore,

$$V_c = 4V_f \approx 2AD\pi. \qquad (11)$$

Or,

$$A \approx V_c/(2D\pi). \qquad (12)$$

By substitution ,

$$P_f = 99 h\nu N_t v (V_c/2D\pi) \frac{\Omega\epsilon}{4\pi} , \qquad (13)$$

or,

$$N_t = \frac{8\pi^2}{99} \frac{P_f}{h\nu} \frac{D}{v} \frac{1}{(\Omega \epsilon V_c)} \cdot \qquad (14)$$

N_t is the only unknown and can be solved for.

The validity of the derivation of N_t depends on the assumption that each atom will radiate 99 times, and that it leaves the laser beam in the metastable state. To verify this assumption, it is necessary to estimate the time required for 99 spontaneous emissions.

Referring to figure 3, $\tau_{31} = 8.2$ns. Therefore the Einstein A coefficient $A_{31} = 1/\tau_{31} = 1.22 \times 10^8 s^{-1}$. The B coefficient for stimulated emission is

$$B_{31} = A_{31} \frac{\pi^2 c^3}{\hbar \omega_o^3} \quad \text{in } m^3/J\text{-}s^2\text{-radian}^3 \qquad (15)$$

where

$\omega_o = 2\pi c/\lambda_o$,
$\lambda_o = 553.5$nm, and
$\hbar$ = Planck's constant/2π

Therefore, $B_{31} = 0.781 \times 10^{22}$ ($m^3/J\text{-}s^2\text{-radian}^3$). The B coefficient for absorption is $B_{13} = 3B_{31}$ since $g_1 B_{13} = g_3 B_{31}$. $g_1 = 1$ and $g_3 = 3$ are the degeneracies of levels 1 and 3. Therefore, $B_{13} = 2.34 \times 10^{22}$ ($m^3/J\text{-}s^2\text{-radian}^3$).

The spectral energy density of the laser above the cathode is

$$\rho = \frac{P}{A_1 \Delta\omega c} \quad \text{in } J\text{-}s/m^3\text{-radian} \qquad (16)$$

where

P is the laser power in W,
A_1 is the beam cross sectional area ($\cong 1.96 \times 10^{-7}$ m^2), and

$\Delta\omega$ is the band width of the laser
$\cong 2.83 \times 10^{11}$ radian/s (Ref 26:3-5).

If P = 100mW, a typical power used in this experiment, then $\rho = 6.01 \times 10^{-15}$ (J-s/m^3-radian).

For an atom in the ground state, the transition rate to the upper level is $B_{13}\rho$. For an atom in level 3, the stimulated transition rate to ground is $B_{31}\rho$, while the spontaneous rate is A_{31}. Therefore, the downward and upward transition rates are $(B_{31}\rho + A_{31})$ and $B_{13}\rho$, respectively. The average time for an atom to cycle once from level 1 to 3 and back to 1 is $1/B_{13}\rho + 1/(B_{31}\rho + A_{31})$. Therefore, the total time for 99 spontaneous transitions is defined as

$$T_{99} = 99 \left[\frac{A_{31} + B_{31}\rho}{A_{31}}\right] \cdot \left[\frac{1}{B_{13}\rho} + \frac{1}{(B_{31}\rho + A_{31})}\right], \quad (17)$$

where

$A_{31}/(A_{31} + B_{31}\rho)$ is the fraction of downward transitions that are spontaneous.

Substituting the appropriate values, $T_{99} \cong 1.8\mu s$.

T_{99} is the same as the estimated 1.8μs transit time for an atom moving through the laser beam. The accuracy of the transit time value depends on the estimates of the atomic velocity and the beam diameter. These values are probably not accurate within ±50%. The derivation of T_{99} depends on an accurate value for the branching ratio. As mentioned previously, the maximum number of photons per atom, on average, can range from 24 to several hundred for slight changes in the branching ratio. Since the estimated

transit time is approximately equal to τ_{99}, it is not clear that all atoms are pumped into the metastable state. However, it is possible. Until more accurate values for v, D, and BR are available, the assumption is made that each Ba atom radiates 99 times on average. This assumption leads to equation 14 for the number density.

One final adjustment must be made to equation 14. In equation 9 the assumption was made that the fluorescent photons could be radiated with equal probability in all directions. In general, resonance fluorescence is anisotropic and will consist of isotropic, electric dipole, electric quadrupole, and magnetic dipole radiations (Ref 27:43-54). However, anisotropy in Ba fluorescence is due primarily to the electric dipole component (Ref 23:237). By measuring the polarization of the fluorescence and knowing the polarization of the incident laser beam, the extent can be calculated to which the fluorescence is anisotropic. Assuming that the detected radiation is partially in an electric dipole pattern, N_t can be multiplied by a correction factor C to account for the anisotropy.

$$C = \frac{2}{3}\,\frac{(1 - \alpha + 3\sin^2\theta)}{(1 + \alpha)\sin^2\theta} \qquad (19)$$

where

θ is the angle between the vertical polarization of the incident beam and the direction of the detected fluorescence (=90° in this experiment), and

α = $I_\perp / I_\parallel$, the ratio of the fluorescent intensities with polarizations perpendicular and parallel to that of the incident beam.

For a derivation of C, see appendix A.

For Ba fluorescence, α is measured to be 0.05. Therefore, $C = 0.70$ and

$$N_t = (0.7)\,\frac{8\pi^2}{99}\,\frac{Pf}{h\nu}\,\frac{D}{v}\,\frac{1}{(\Omega\epsilon V_c)} \quad \text{in Ba atoms/m}^3. \tag{19}$$

Equation 19 is the principal result of this chapter. For the geometry of this experiment, equation 19 relates the Ba number density to the measured fluorescent intensity.

IV Equipment and Procedures

This chapter describes the equipment used to detect Ba atoms. A laser was used to produce radiation to excite the Ba. A wavelength calibration system was needed to assure that the laser was tuned to precisely the Ba 553.5nm transition. The beam had to be directed through a vacuum cell containing a dispenser cathode evaporating Ba atoms. Some of the atoms passed through the laser beam, producing fluorescence. Finally, the fluorescent photons had to be collected and diverted into a photomultiplier tube (PMT) for detection and counting.

Laser

A Spectra Physics model 164 argon ion laser was used to pump a Spectra Physics model 375 continuous wave dye laser. The pump laser was operated on all available lines and produced up to 3.5W of power. The dye laser was used with Rhodamine 560 dye and could be tuned continuously from 540 to 575nm. The maximum power output with no tuning elements in the dye laser was 340mW at 549nm. Two tuning elements used were a wedge for coarse tuning and an etalon for fine tuning. When both were used, the maximum power available at 553.5nm, the Ba resonance, was 190mW. In previous work by Benham to detect Na fluorescence, a Spectra Physics model 370 dye laser had been used. In the present study, the model 375 was used because it yielded a higher power and had better frequency stability. An examination of the mode structure

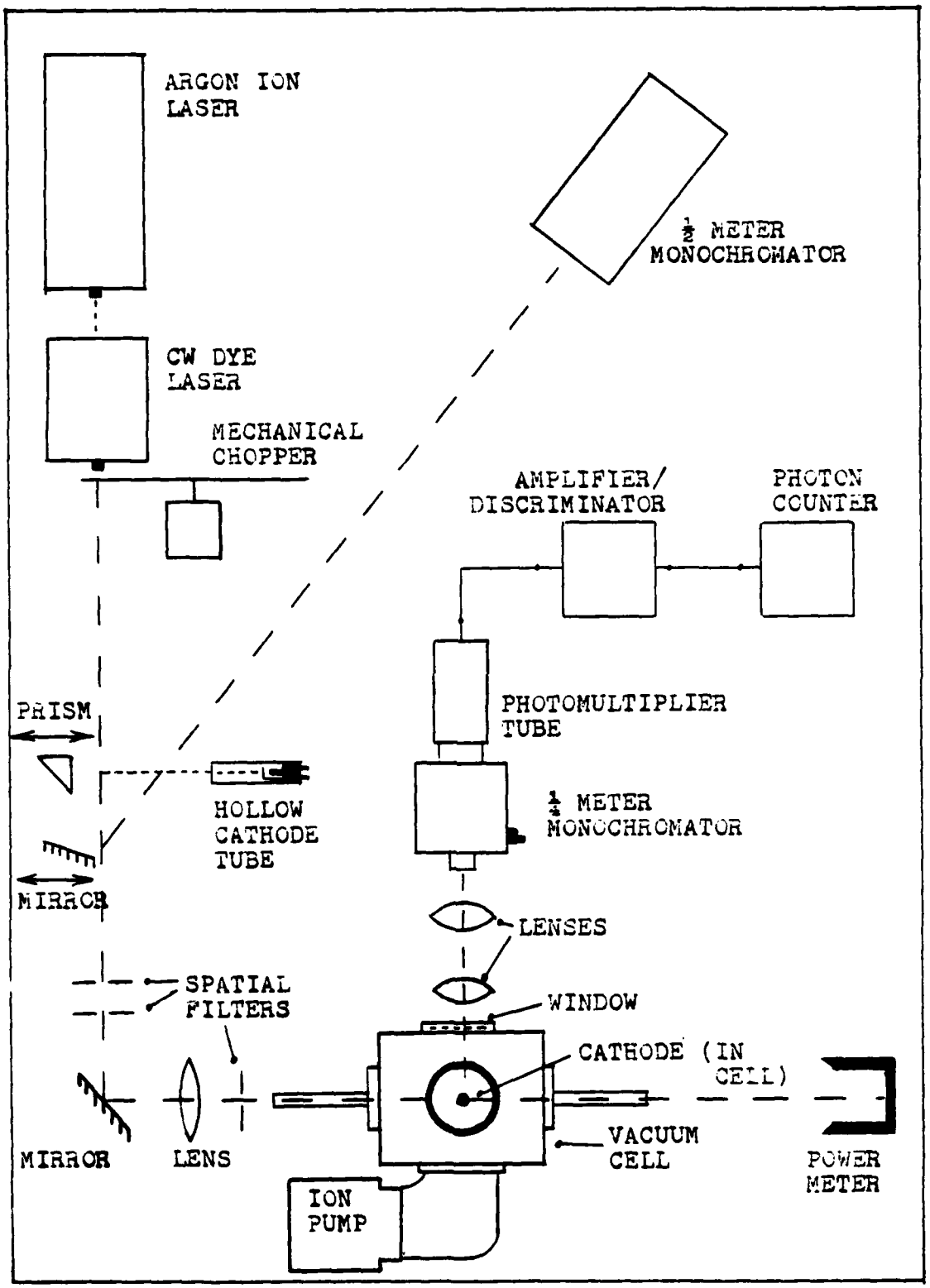

Figure 5. Diagram of Apparatus

with a Fabry-Perot interferometer showed little tendency for the model 375's radiation to jump between modes.

Using the wedge without the etalon, the dye laser could be tuned continuously over its range. With the etalon in place, and tuning done with the wedge, the dye laser radiation would jump from one etalon mode to the next. With both elements in place, Rotating the etalon would scan the laser through a range of 1.0nm. Therefore, the best method of tuning was to set the wedge so that the laser was at approximately the correct wavelength, then insert the etalon for fine tuning. With both elements in use, the laser cavity mode separation of the dye laser was 900GHz at 580nm, or 1.0nm (Ref 26:3-8).

The laser beam was horizontally polarized at the dye laser output. However, a beam steering device used to lower the beam and turn it 90° changed the polarization to vertical as the beam entered the test cell. This steering mechanism also was used to make fine adjustments to the direction of the beam as it passed through the test cell. Before entering the cell, the beam passed through several spatial filters and a lens that focused it above the cathode. After exiting the test chamber, the laser power was measured using a calorimetric power meter.

The Optogalvanic Effect Applied to Laser Tuning

In order to induce fluorescence in the Ba atoms above the cathode, the laser had to be tuned precisely to the Ba 553.5nm line. Laser radiation in resonance with the Ba

transition can interact with Ba in a gaseous discharge to alter the voltage and current characteristics of the discharge. Detection of this optogalvanic effect provided a method for setting the laser wavelength.

Optogalvanic detection requires the use of a Ba hollow discharge tube, shown in figure 6. The cathode of this tube is a hollow metal cylinder. The tube is filled with an inert Ne buffer gas. When a DC voltage is applied between anode and cathode, a discharge starts in the Ne. If the voltage is raised, the discharge current will increase, and Ne atoms will begin sputtering Ba atoms from the wall of the cathode. In this way, Ba begins to participate in the discharge.

If a laser beam is directed into the discharge it may interact with atoms in several ways. It could ionize atoms that have been collisionally excited. Or the laser could excite atoms, allowing them to be collisionally ionized. Either process would raise the discharge current and lower the discharge voltage. Finally, the laser could depopulate a metastable level that had been collisionally excited. This would increase the discharge voltage. The second and third interactions would only occur if the laser were tuned to a transition frequency of one of the species in the discharge. If the laser beam does interact with one of the species in the discharge, the current and voltage characteristics of the discharge will be changed. This is the optogalvanic effect (Refs 28 and 29).

The optogalvanic effect can be detected by monitoring

the voltage across the hollow cathode tube. The changes in the voltage are easier to detect if they occur periodically. Therefore, the laser beam was chopped at a set frequency, then sent into the bore of the hollow cathode. A magnetic pick up on the hub of the chopper wheel produced a signal sent to the photon counter. The 'chop monitor' output of the photon counter was a square wave used to trigger an oscilloscope. The photon counter will be discussed in more detail later. For now one need only know that it was used to process the chopper signal into a clean triggering signal for the oscilloscope. The anode of the tube was connected to the oscilloscope through a coupling capicitor so that only fluctuations in the discharge voltage would be passed. See figure 7 for an electrical schematic of the wavelength calibration system. When the laser was tuned to a resonance in either Ba or Ne, the discharge voltage would change and a signal would appear on the scope similar to the one shown in figure 8.

Since the discharge contained both Ba and Ne, it was necessary to distinguish the optogalvanic signal of Ba from those of the many Ne lines within the tuning range of the laser. To do this, the Ne lines were used as a calibration spectrum. The laser was scanned through its range and a set of optogalvanic signals were located. When a signal was found, the beam was diverted into a half meter monochomator to roughly determine the wavelength. Then the set of wavelengths was compared to a table of Ne transitions and the detected lines were identified (Ref30:204-205). Two of the

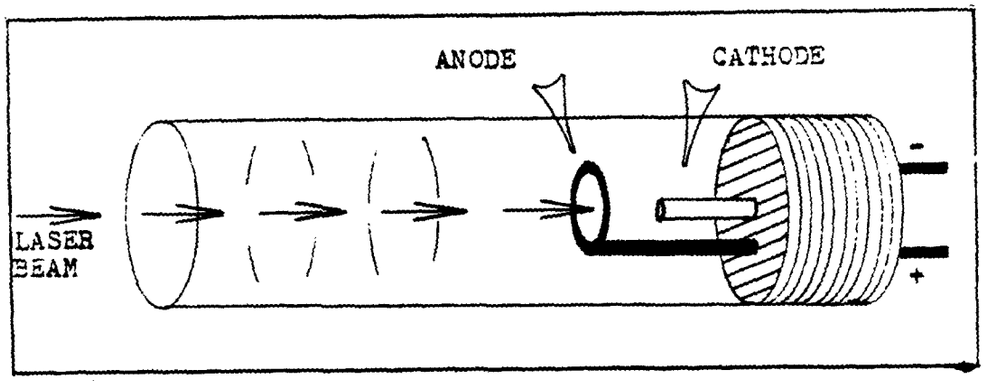

Figure 6. Hollow Cathode Discharge Tube

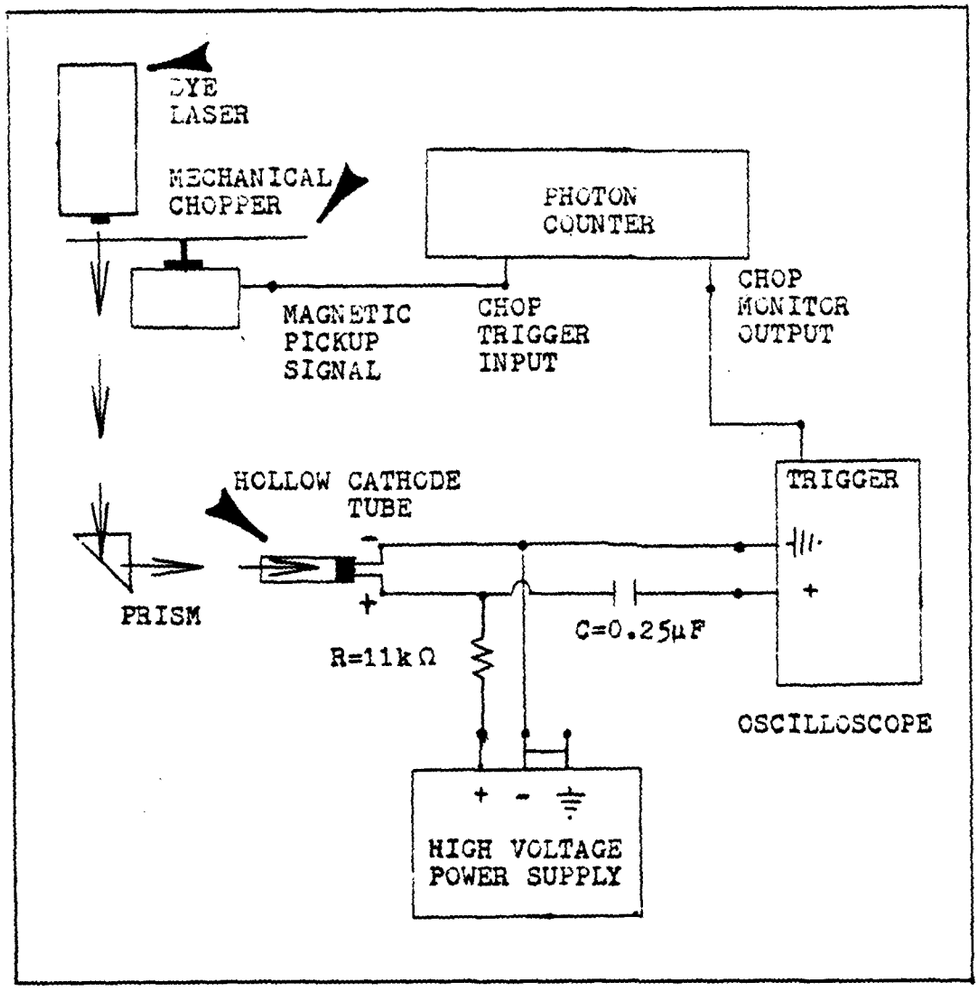

Figure 7. Schematic Diagram of
Wavelength Calibration System

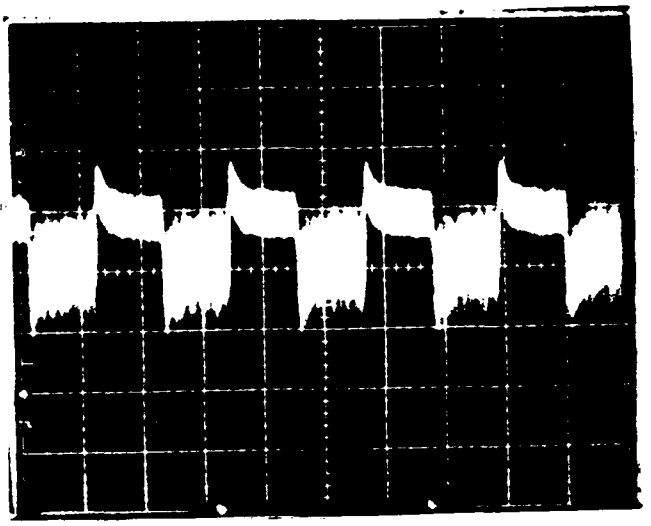

Vertical Scale: 5mV/cm
Horizontal Scale: 5ms/cm

Figure 8. Typical Optogalvanic Signal from Ba (553.5nm)

Ne lines found in the scan were at 553.37nm and 553.87nm. A slow scan between these lines located the Ba 553.5nm line. All three lines could be found by scanning with the etalon because they are within the free spectral range of the etalon (1.0nm). Having the resonance bracketed by two Ne lines made locating the Ba line simple. Minor adjustments to the wavelength were made by slowly rotating the etalon until the detected fluorescent intensity was maximized.

The greatest disadvantage of this wavelength calibration method was that the entire beam had to be diverted into the hollow cathode tube to produce a detectable signal. Therefore, tuning couldn't be checked while an experiment was in progress. However, the optogalvanic effect provided a

convenient method for setting the laser wavelength.

Vacuum Cell

The vacuum cell provides a high vacuum environment in which to test the dispenser cathode. If the cathode were exposed to atmosphere, it would probably be contaminated by water vapor and other compounds that could be adsorbed onto its surface. Although the impregnated dispenser cathode is more recoverable from poisoning than the oxide film cathode, caution dictates leaving it in as high a vacuum as possible. One report indicates that at a pressure of 10^{-7} torr, poisoning effects are noticeable but do not severely impair cathode operation (Ref 5:398-399). Maintenance of a high vacuum during an experiment is important both to minimize cathode poisoning and to allow collisional de-excitation of Ba atoms to be neglected.

The pumping system for the cell consists of two cryogenic adsorption pumps and an ion pump. The adsorption pumps reduce the pressure to below 10^{-3} torr. Then the ion pump can be started. It maintains the vacuum near 10^{-7} torr. If a cold finger in the cell is cooled with liquid nitrogen, the pressure can drop to near 10^{-9} torr. The purpose of the cold finger is to trap as much material as possible that is evaporated from the cathode. When an experiment is being run, with the cathode heated to about 1000°C, the pressure rises to 1.5×10^{-7} torr. This pressure is sufficiently low that collisional de-excitation is negligible.

A leak valve to the chamber allows backfilling from

some gas reservoir. Normally this valve is used to flow nitrogen gas into the chamber for the calibration measurements. For these measurements, Rayliegh scattered laser radiation from the N_2 molecules is detected and used to determine the constants $\Omega\epsilon V_c$ introduced in the last chapter. See appendix B for a description of the calibration process.

The cathode used is a Semicon Type "S", impregnated with a 4:1:1 mixture of BaO: CaO: Al_2O_3 (Ref 6). It is mounted in the cell so that its surface is horizontal and directly below the beam. Since the cathode needs electrical connections for its heater, it is mounted on a flange with wire feed throughs. This flange is attached to a bellows that is attached to a port in the chamber. The bellows may be expanded or contracted by adjusting the threaded rods holding it in place. (See figure 9). In this way the cathode can be moved up and down and tilted slightly to any side.

A glass port in front of the cathode allows viewing at right angles to the laser beam. Viewing the cathode through this port with an optical pyrometer allows the temperature of the cathode to be determined. Experiments were performed with the cathode temperature ranging from 900 to 1050°C. This port also allows the detection optics to collect the resonance fluorescence of the cathode effluents.

Detection Optics and Electronics

In order to determine Be concentretions, the intensity of the resonance fluorescence had to be measured. This was

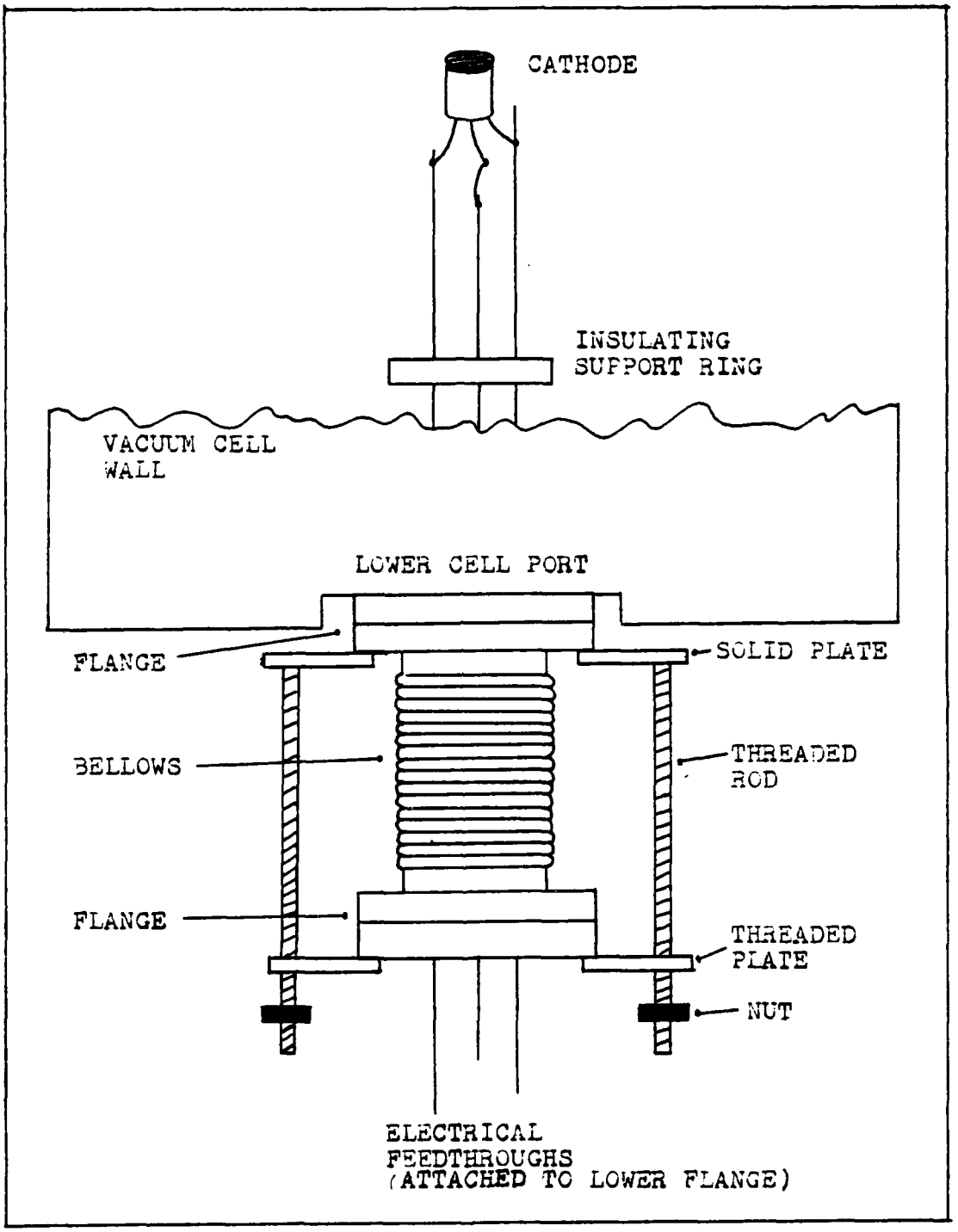

Figure 9. Bellows Arrangement for Adjusting Cathode Position

done by collecting a fraction of the fluorescent light into a photomultiplier tube (PMT). The output of the PMT was processed by photon counting electronics to give a measure of the number of fluorescent photons. The detection system was also used to measure the background contributions from various sources.

Two lenses outside the viewing port of the vacuum cell on an axis at right angles to the laser beam were used to focus the image of the fluorescing volume onto the entrance slit of a quarter meter monochromator. The lenses were chosen so that the image would diverge past the entrance slit until it just filled the collimating mirror of the monochromator. The monochromator was used to filter some of the blackbody radiation from the heated cathode. This was necessary to keep the noise from swamping the fluorescent signal and overloading the detector. The exit slit of the monochromator was coupled directly to the PMT housing. The coupling provided a light seal around the PMT and brought the PMT photocathode as close to the exit slit as possible. This ensured that nearly all of the photons leaving the exit slit struck the photocathode.

The PMT used was a RCA 8850, which was designed for photon counting systems. Thermionic emission from the photocathode at room temperature caused approximately 300 dark counts per second. This was the number of counts detected when the photocathode intercepted no photons. Using a thermoelectric cooler to cool the photocathode to -25°C, the dark count was reduced to 90 per second.

Pulses from the PMT went through an amplifier to a discriminator. The lower discriminator level was set to eliminate electronic noise. The upper discriminator level wasn't used. Therefore, the detection system counted all pulses with amplitude above the lower discriminator level. If either the PMT or the discriminator were overloaded, then each pulse passing the discriminator corresponded to one emission from the photocathode.

Pulses passing the discriminator went to a Princeton Applied Research model 1112 Photon Counter. The counter had several modes which made it a versatile piece of equipment. Most of the experiment was done with the counter in the background subtract mode. In this mode the light chopper was used so that the sample volume was alternately illuminated and darkened. A photocell intercepted reflections of the laser beam from the entrance Brewster window of the vacuum cell and provided a signal to trigger the counter. Recall that the chopper also provided a magnetic pick up signal used to trigger the oscilloscope during tuning. However, the photocell signal was more reliable because it actually corresponded to when the laser beam entered the vacuum cell. With the trigger signal as an input, the counter generated a timing signal similar to that shown in figure 10.

During the half cycle that the laser was blocked, the counter would receive pulses into a register for a preset sampling interval less than the half cycle time. These counts were background counts. During the next half cycle,

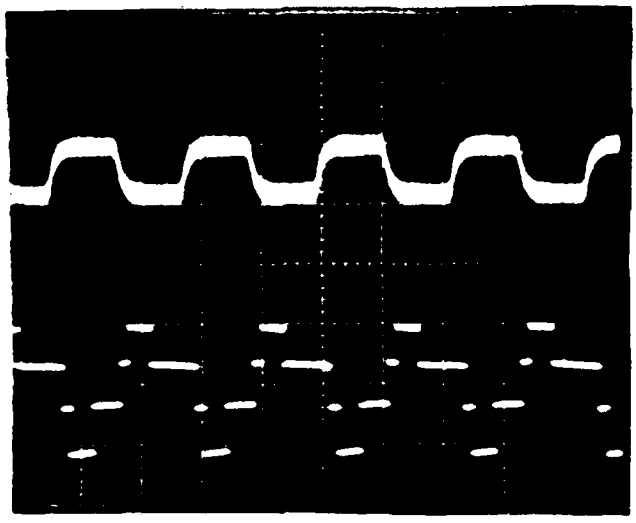

TOP: Photocell pickup from first Brewster window

BOTTOM: Timing signal from photon counter 'chop monitor' output

Figure 10. Timing Trace for Synchronous Background Subtraction

pulses would accumulate in another register for the same time period. Since the laser would have been unblocked during that time, those counts were background plus signal. The counter would continue this process for a preset number of cycles. The total sampling time for either register was the sampling interval per half cycle times the number of cycles. The counter display included the contents of both registers and their sum and difference. The difference was the signal caused by laser illumination. Included in that signal were resonance fluorescence from Ba, and scattering from the surroundings and other vapor constituents. The sum was the total number of counts. Assuming Poisson stat-

istics, the standard deviation of the signal would be the square root of the total number of counts. Therefore, the photon counter was used to simultaneously measure the constant background, the laser induced signal, and the fluctuation of the signal.

Procedures

The previous sections of this chapter give much of the detail of how individual pieces of equipment operate. This section outlines the general procedures used in the experiment. Recall that the purpose of the experiment was to measure the concentration and evaporation rate of Ba from a heated dispenser cathode as a function of temperature. If the evaporation rates of Ba and other species such as BaO and Ca were known as functions of temperature and current density, then better models of cathode operation might be developed. This effort is limited to using resonance fluorescence to measure Ba concentrations.

The procedure was designed to allow measurements of the intensity of the Ba fluorescence while keeping several variables constant. The three most important variables that needed to be controlled were laser power, laser frequency, and cathode temperature. Laser power was continuously monitored by sending the beam into a power meter as it left the test cell. Minor adjustments could be made to the laser power during a run. The laser frequency could not be continuously monitored. It had to be set on resonance using the optogalvanic signal, then checked period-

ically during the course of the experiment. The frequency changed slightly whenever the power changed, and therefore had to be adjusted. Minor adjustments to the frequency could be made by rotating the etalon slowly until the number of fluorescent counts in a short time period was peaked. Finally, cathode temperature was kept constant by monitoring the number of background counts in some time period and adjusting the heater current if necessary. Temperature variation wasn't a great problem because the heater power supply provided a steady current.

The most important part of the experiment consisted of measuring the fluorescent intensity at several temperatures and for a range of laser powers. A set of measurements at one temperature could be used to calculate the Ba concentration at that temperature. With the cathode temperature and laser power set, the photon counter alternately sampled (background) and (signal + background) pulses for a preset time. The time had to be long enough so that the statistical variation of the total number of counts was small compared to the number of signal counts.

The counts accumulated in the background register represented the intensity of light seen by the PMT independent of laser illumination. The principal source of this continuous background was the thermal radiation from the cathode.

Of the signal produced by laser irradiation, not all was resonance fluorescence of Ba. Some was scattering from the cathode and other surroundings, and some was scattering from other species in the vapor. Elastic scatter from vapor

constituents was measured by tuning the laser slightly off resonance with the cathode heated. Then the signal consisted not of fluorescence, but of scatter from the surroundings and the vapor. The values of the various background contributions had to be known to extract the fluorescence intensity from the data. Then from the fluorescence intensity, the Ba concentration and evaporation rate could be calculated using equation 19. The results of these measurements are presented in the next chapter.

V Results

The principal results of this experiment are the values of fluorescent intensity measured as functions of cathode temperature and laser power. Derived from these data are values of Ba concentration, evaporation rate, and flux as functions of cathode temperature. In order to extract fluorescent intensity from the recorded data, several sources of background had to be identified and measured. This chapter presents the background estimates and the calculated values of Ba concentration.

Background

Among the several sources of background, the most prominent was the thermal radiation from the cathode. Another constant source was the dark current from the photomultiplier. In addition, two other sources depended on the intensity of the laser irradiation. They were the scatter from surroundings and vapor components. Methods of counting statistics had to be used to extract estimates of the various backgrounds from the data. What follows is a review of counting statistics, then discussions of each of the background contributions.

Counting Statistics. The time interval between events producing counts in a detector is assumed to be randomly distributed about some mean value, $\bar{r}$. The random distribution is often assumed to be a Poisson distribution if the

number of events is large. For a Poisson distribution, the variance $\sigma^2 = \bar{x}$. If a single measurement of x counts is taken, then x is assumed to be the mean because it is the only value available. Then the sample variance s^2 is approximated as x. If several measurements are taken, then s^2 can be calculated. If the process is actually a Poisson process, then $s^2 = \sigma^2$.

For a Poisson distribution about $\bar{x}$, the standard deviation is $\sigma = \sqrt{\bar{x}}$. In the experimental case, where only one or a few measurements are taken, the best estimate of the standard deviation is $\sqrt{s^2} \cong \sqrt{x}$, where x is the measured mean. If the mean value is large enough for the distribution to be Gaussian, then 68% of all measured values should be within $\pm\sigma$ of the mean. Also, 90% of all values should be within $\pm 2.58\sigma$ of the mean. We can apply this to the experimental situation by saying that the actual sample mean, which would be found from a large number of measurements, is within the range $x \pm 2.58\sqrt{x}$ 90% of the time. Again, x is the estimate of the mean based on the available data.

Caution should be taken that the estimate of σ is applied only to a number of detected counts. It can't be applied to sums, differences, or averages of counts, or count rates. The standard deviation of a sum or difference $C = A \pm B$ is $\sigma_C = (\sigma_A^2 + \sigma_B^2)^{\frac{1}{2}}$. The standard deviation of a counting rate of x counts in t seconds is $\sigma_R = \sigma_x/t$. Therefore, the deviation in the count rate drops as counting time increases, for constant rate.

For a more complete review of counting stastics, see Bevington or Knoll (Refs 31,32:104-147).

Background from the Cathode. Noise from the cathode was independent of laser irradiation and therefore was subtracted by the counter. But the deviation of this background influenced the deviation of the measured fluorescent signal. Since the photon counter alternately counted background and (background + signal), the variance of the signal is estimated to be

$$\sigma_s^2 = (BG)^2 + (BG + SIG)^2 \quad , \tag{20}$$

where

BG is the recorded background, and
SIG is the signal.

In every case recorded in this experiment, the deviation of the background was negligible compared to the fluorescent signal. In the worst case (10mW, 925°C) the ratio of σ_s to the signal was 3×10^{-3}. The actual deviation in a set of measurements taken for the same interval was larger than the estimate based on statistics. This is probably due to the inability to maintain cathode temperature, and laser power and frequency at constant values. However, the actual deviation was still negligibly small for every set of data.

Although the deviation of the cathode background was small, for many measurements, the actual background was in the same order of magnitude as the fluorescent signal. Figure 11 shows the signal to background ratio as a function

of cathode temperature for several laser powers. A peak is reached near 1000°C, indicating that at lower temperatures, the signal is small, but at higher temperatures, the background is large. The blackbody noise gains intensity with temperature more rapidly than the fluorescent signal.

Background from the Dark Current. As mentioned in chapter IV, the dark count rate was 90 per second. Since the lowest fluorescent count rate was 31,000 per second, dark noise was negligible.

Background from Scatter from Surroundings. Figure 12 shows the scattered count rate as a function of laser power. A least squares fit of these points gives a linear correlation coefficient of 98.9%. Again, compared to fluorescent count rates, this scatter is negligible.

Background from Scatter from the Vapor. As described in chapter IV, the scatter from surroundings and vapor was determined in one measurement. Since the scatter from surroundings was determined independently, scatter from the vapor could be extracted. Figure 13 shows the rate of scatter from the vapor as a function of laser power at several temperatures. The scattered intensity from the vapor increases roughly linearly with laser power. Because of low count rates, the statistics were not good enough to determine whether the scattered intensity changed with temperature. It is expected to, since the vapor pressure of the cathode should increase with temperature. The intensity scattered from the vapor can be considered negligible compared to the fluorescent intensity.

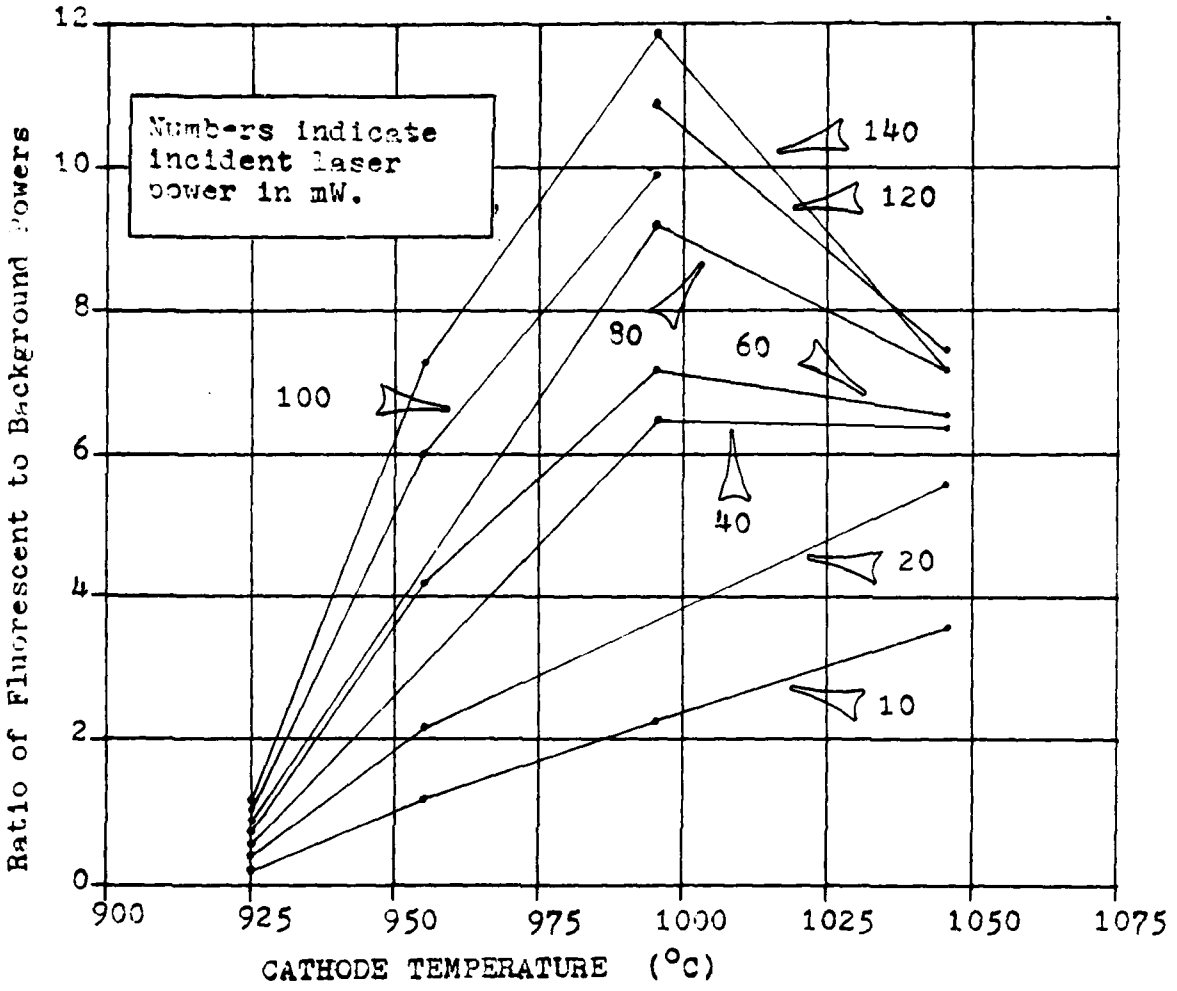

Figure 11. Graph of Signal to Noise Ratio vs. Cathode Temperature for Several Laser Powers

Fluorescent Intensity

Figure 14 shows the principal data of this experiment. It is a graph of the fluorescent count rate as a function of laser power for several cathode temperatures. Not all of these curves clearly saturate, but they approach a saturation level that can be approximated. Recall from chapter III that saturation was possible since each Ba atom was assumed to radiate only 99 times, on average. From the estimates

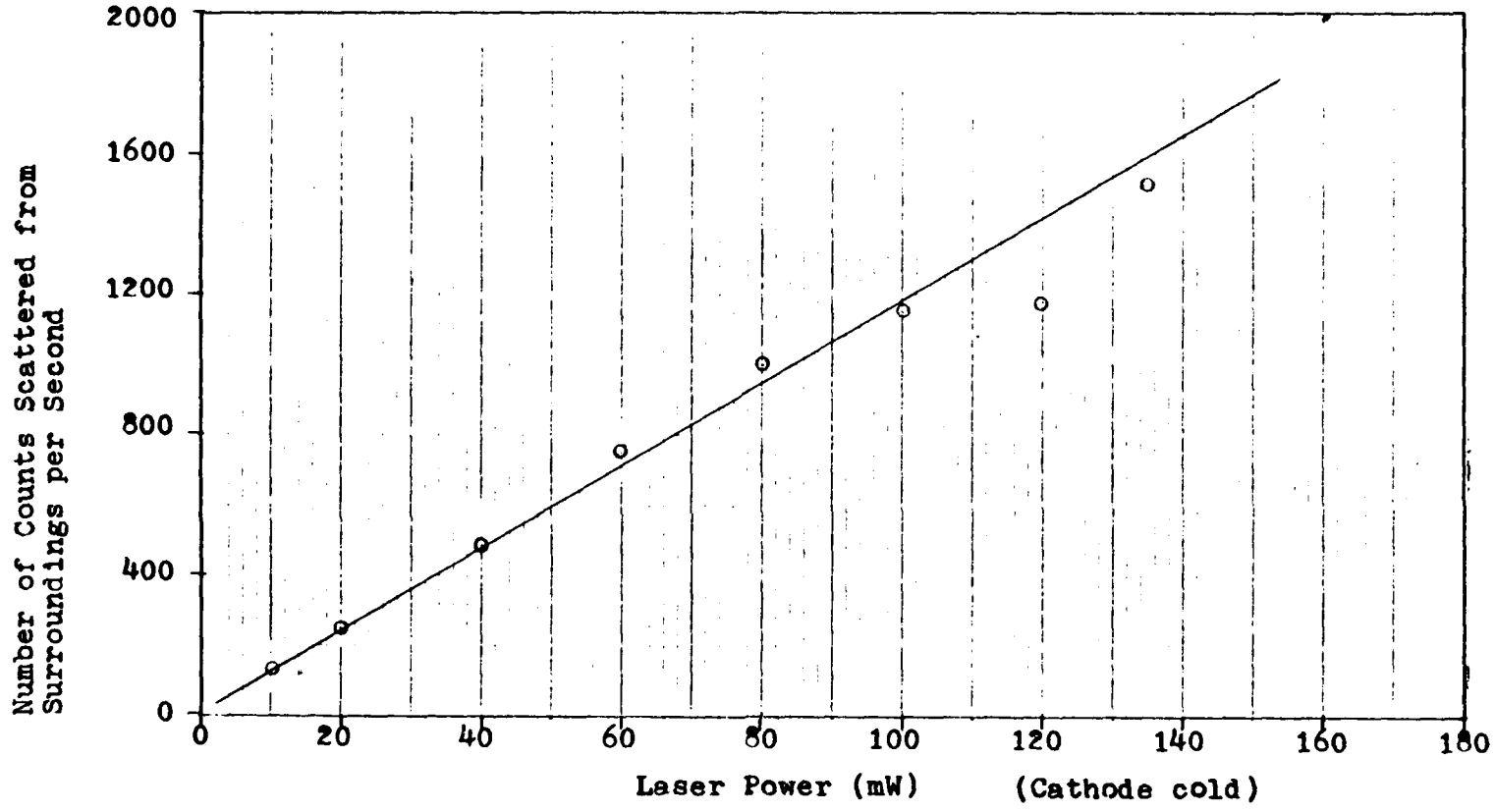

Figure 12. Rate of Scatter from Surroundings vs. Laser Power

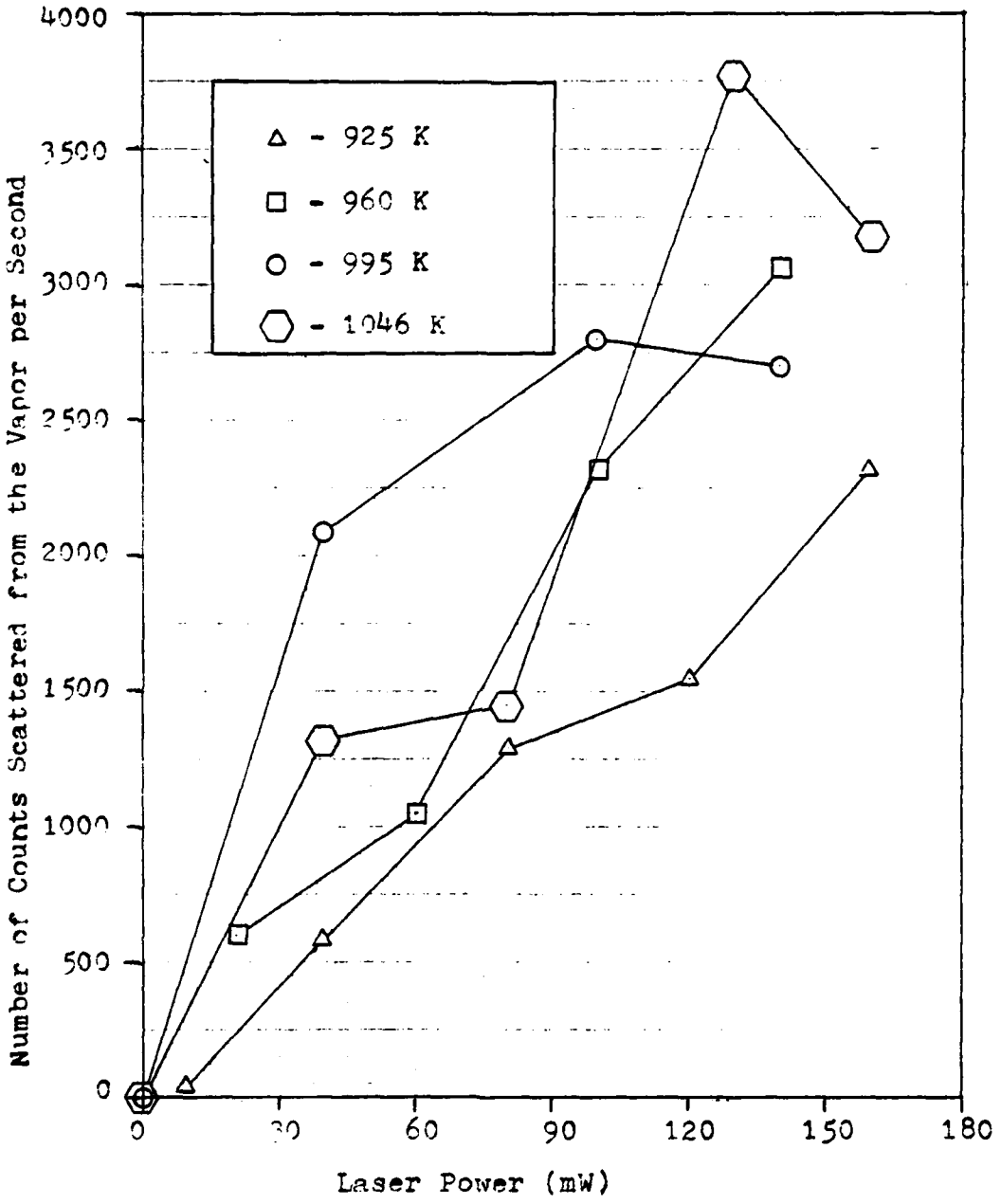

Figure 13. Rate of Scatter from Vapor vs. Laser Power for Several Cathode Temperatures

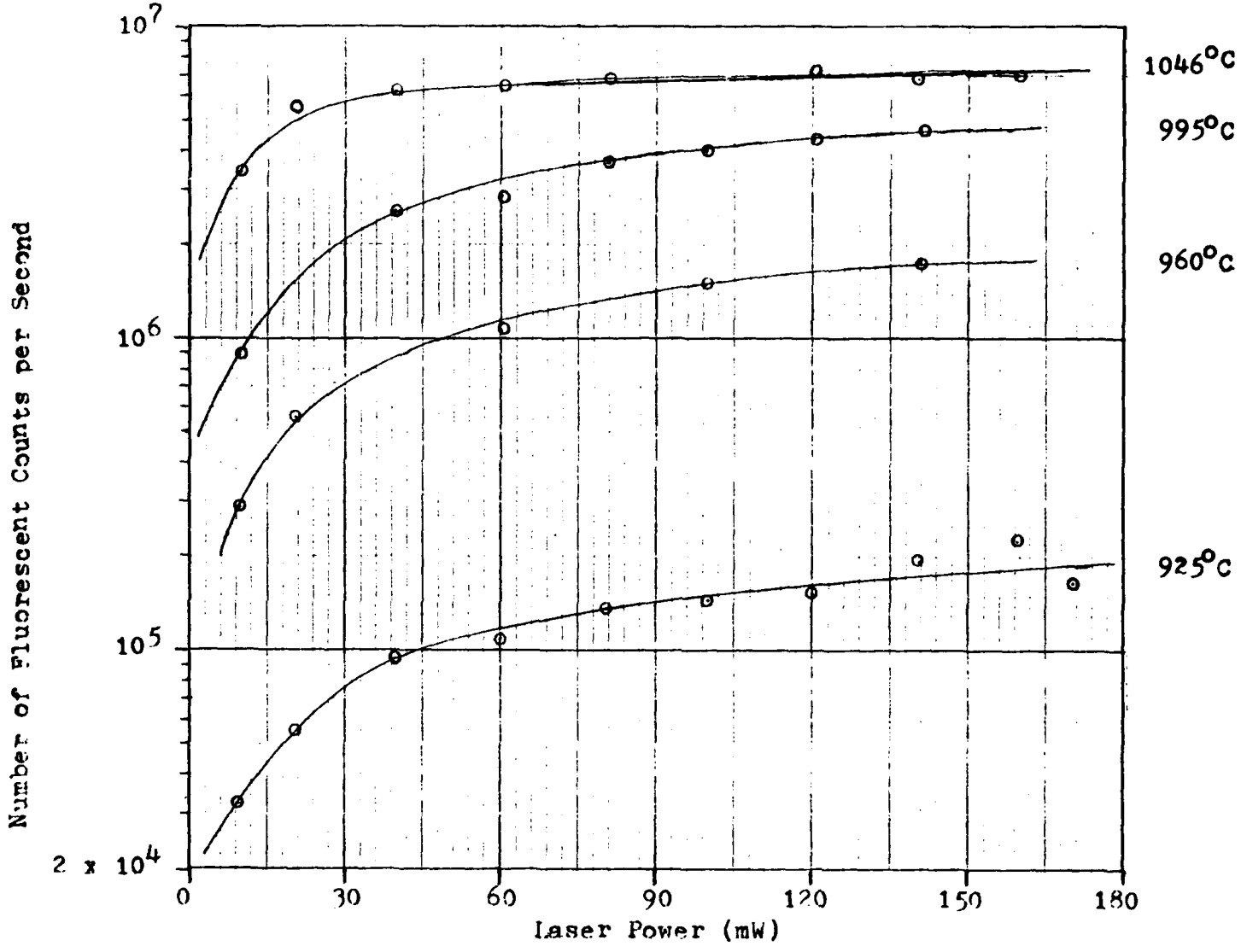

Figure 14. Fluorescent Intensity vs. Laser Power for Several Temperatures

of the saturated fluorescent intensities, the Ba concentration can be calculated for each temperature.

The curves in figure 14 are somewhat peculiar in that saturation does not occur more quickly at lower temperatures as would be expected because of the lower Ba density. In fact the curve for 1046°C saturates at the lowest power. Since no experimental conditions are believed to have caused this result, the saturation intensities are assumed to be correct and are used to calculate the Ba concentrations.

Ba Concentrations and Evaporation Rates

Table 1 shows the measured fluorescent power, P_f, as a function of temperature. Using equation 19, the evaporation flux can be estimated assuming 1) that the concentration is constant over the cathode surface, and 2) that the atoms travel at the speed v = 280m/s. Then,

$$F_e = N_t v \quad \text{in atoms/m}^2\text{-s} \tag{21}$$

where

F_e is the evaporation flux.

To calculate the evaporation rate, an estimate must be made of the area through which that concentration is flowing. The assumption is made that all atoms move vertically from the cathode. Therefore, $R_e = F_e A_c$, where R_e is the evaporation rate and A_c is the cathode area. $A_c = 4.56 \times 10^{-9} m^2$. This estimate of R_e is low since some atoms will move horizontally from the surface of the cathode. However, since the beam passes within one cathode diameter of the cathode

TABLE I: Ba Evaporation Rates and Related Quantities as Functions of Temperature

Cathode Temperature T(K)	Detected Fluorescent Power (W) (saturated)	Ba Number Density (m^{-3})	Ba Flux from Cathode ($\frac{\#\ atoms}{m^2\text{-}s}$)	Rate of Ba Evaporation (# atoms/s)
1046	2.4×10^{-12}	6.1×10^{12}	1.7×10^{15}	7.8×10^{10}
995	1.7×10^{-12}	4.3×10^{12}	1.2×10^{15}	5.4×10^{10}
960	8.4×10^{-13}	2.1×10^{12}	5.9×10^{14}	2.7×10^{10}
925	6.3×10^{-13}	1.5×10^{12}	4.5×10^{14}	2.0×10^{10}

surface, the assumption of vertical motion is acceptable. Values for F_e and R_e are in Table 1.

Figure 15 shows the variation of evaporation flux with cathode temperature. The error bars show estimates of the uncertainty in determining the saturation level of the fluorescent intensity from figure 14. From these points, a reliable expression for evaporation rates as functions of temperature cannot be determined. Measurements at more temperatures would be required.

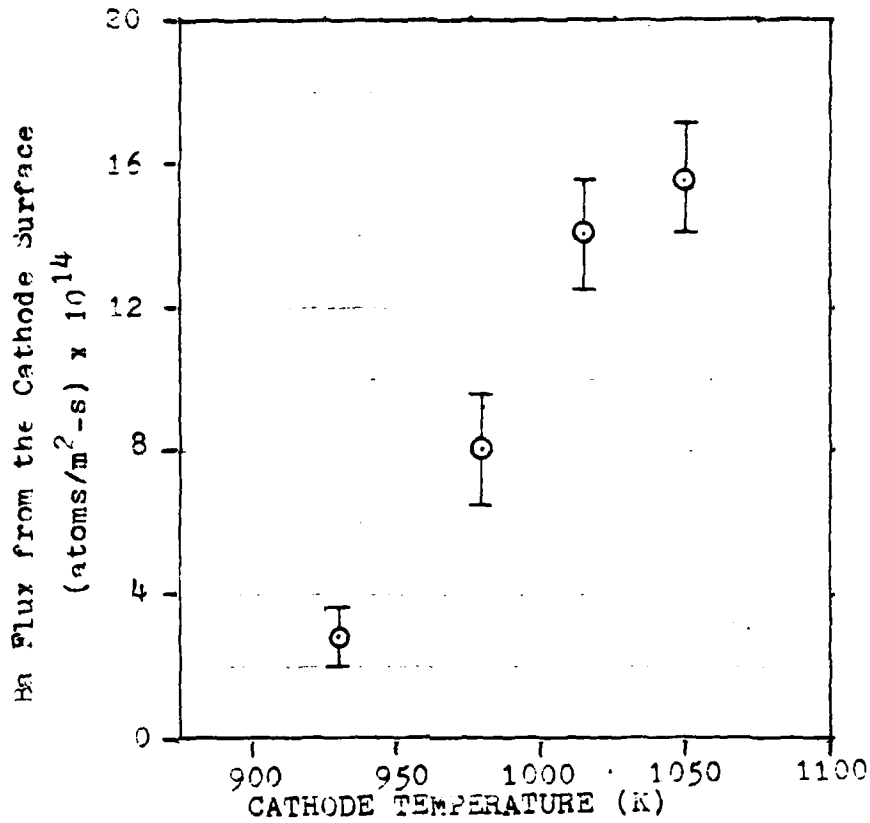

Figure 15. Ba Flux vs. Cathode Temperature

Comment on Accuracy

The determined values for evaporation rates depend on the validity of several assumptions and approximations which are summarized below..

1) The rms speed of the Ba atoms was assumed to be 280m/s using a Maxwellian distribution at the cathode temperature.

2) The beam diameter above the cathode was visually estimated to be 0.5mm ± 25%. An inaccurate measurement would have affected the calculated fluorescing

volume.

3) The calibration method used to determine $\Omega V_c \epsilon$ was assumed to be correct. It depended on having the correct value for the differential scattering cross section of N_2 gas. In this study, an experimental value from the literature was used.

4) In determining the fluorescing volume and evaporation rates, Ba atoms were assumed to migrate vertically from the cathode. However, some atoms moved horizontally and the Ba density could not have been constant in all directions.

5) The branching ratio would only have to be slightly different from 99% to the $^1S_0$ state for the maximum number of photons per atom to have been much different from 99. If BR were < 99%, then the signal could be assumed to saturate at a lower number of photons per atom. If BR were >99%, then the number of photons per atom could be limited by the beam transit time and not pumping into the metastable state.

VI Conclusions

This effort demonstrated that the density of Ba evaporating from the dispenser cathode could be measured using laser induced resonance fluorescence. The technique could be used to monitor Ba evaporation as a function of temperature over the cathode life.

Several specific conclusions can be drawn from the experimental work.

1) The Ba fluorescence saturates or comes close to saturating at less than 170mW of laser power, for the cathode temperatures used.

2) The Ba number density can be calculated from the fluorescent intensity by assuming that since Ba has a metastable state, each atom will radiate 99 times, on average.

3) The Ba density increases with the cathode temperature. The functional relation is not known.

4) Of the various background sources, thermal radiation from the cathode is the most prominent. Its effect can be minimized by using synchronous background subtraction.

5) The ratio of the fluorescent intensity to the intensity from the cathode background reaches a maximum at about 1000°C.

VII Recommendations

The technique of fluorescence detection shows promise for determining the densities of effluents from dispenser cathodes. However, several quantities must be determined more accurately to be able to derive atomic number density from fluorescent intensity. They are listed bellow.

1) The atomic velocity affects estimates of the beam transit time.

2) The beam diameter affects estimates of both the transit time and the fluorescing volume.

3) The branching ratio affects estimates of the number of fluorescent photons per atom.

By examining the evaporated quantities of various cathode components, impregnant depletion mechanisms, cathode chemistry, and the nature of the emitting surface may be determined. Using resonance fluorescence, several experiments could be performed on the evaporated species of dispenser cathodes.

1) Measure the Ba evaporation rate as a function of time for a set temperature.

2) More thoroughly measure the Ba evaporation rate as a function of temperature.

3) Install an electron collection anode and measure the Ba evaporation rate as a function of current density.

4) Search for BaO by searching for BaO resonances. Then perform the tests in 1-3 .

5) Change to an appropriate laser dye and make the same measurements for Ca. This may explain the role of Ca in increasing emission.

Bibliography

1. Kittel, Charles. Introduction to Solid State Physics. New York: John Wiley & Sons, Inc., 1976.

2. Forman, Ralph. "A Proposed Physical Model for the Impregnated Tungsten Cathode Based on Auger Surface Studies of the Ba-O-W System," Applications of Surface Science,2: 258-274 (1979).

3. Kohl, Walter H. Materials and Techniques for Electron Tubes. New York: Reinhold Publishing Corp., 1960.

4. Jenkins, R.O. "A Review of Thermionic Cathodes." Vacuum,19: 353-359 (August 1969).

5. Strauss, Robert, J. Bretting, and R. Metivier. "Travelling Wave Tubes for Communication Satellites," Proceedings of the IEEE, 65: 387-400 (March 1977).

6. Technical Bulletin. Subject: Semicon Dispenser Cathodes. Semicon Associates, Inc.

7. Venema,A., R.C. Hughes, P.P. Coppola, and R. Levi. "Dispenser Cathodes," Philips Technical Review, 19: 177-190 (December 1957).

8. Rittner, E.S., R.H. Ahlert, W.C. Rutledge. "Studies on the Mechanism of Operation of the L Cathode. I," Journal of Applied Physics, 28: 156-166 (February 1957).

9. Levi, Roberto. "New Dispenser Type Thermionic Cathode," Journal of Applied Physics, 24: 233 (1953).

10. Rittner, E.S, W.C.Rutledge, and R.H. Ahlert. "On the Mechanism of Operation of the Barium Aluminate Impregnated Cathode," Journal of Applied Physics,28: 1468-1473 (December 1957).

11. Palluel, P., and A.M. Shroff. "Experimental Study of Impregnated Cathode Behavior, Emission, and Life," Journal of Applied Physics, 51: 2894-2902 (May 1980).

12. Rittner, E.S. "On the Mechanisms of Operation of the Type B Impregnated Cathode," Journal of Applied Physics, 48: 4344-4346 (October 1977).

13. Brodie, I., and R.O. Jenkins. "The Nature of the Emitting Surface of Barium Dispenser Cathodes," British Journal of Applied Physics, 8: 27-29 (January 1957).

14. Brodie, I., and R.O. Jenkins, and W.G. Trodden. "Evaporation of Barium from Cathodes Impregnated with Barium-Calcium- Aluminate," Journal of Electronics and Control, 6: 149-161 (February 1959).

15. Forman,Ralph. "Surface Studies of Barium and Barium Oxide on Tungsten and Its Application to Understanding the Mechanism of Operation of an Impregnated Tungsten Cathode," Journal of Applied Physics, 47: 5272-5279 (December 1976).

16. Forman, Ralph. "Comment on the Mechanism of Operation of the Imoregnated Tungsten Cathode," Journal of Applied Physics, 50: 1546-1547 (March 1979).

17. Haas, G.A., H.F. Grey, and R.E. Thomas. "Effects of S, Ba, and C on Impregnated Cathode Surfaces," Journal of Applied Physics, 46: 3293-3301 (August 1975).

18. Mitchell, Allen C.G., and Mark W. Zemansky. Resonance Radiation and Excited Atoms. London: Cambridge University Press, 1934.

19. Fairbank, W.M., and C.Y. She. "Single-Atom Detection with Lasers," Optics News, Spring 1979: 4-8.

20. Balykin, V.I., V.S. Letokhov, V.I. Mishin, and V.A. Semchishen. "Laser Detection of Single Atom Fluorescence," JETP Letters, 26: 357-359 (September 1977).

21. Lurig, Allen. "Lifetime of the First Excited $^1P_1$ State of Mg and Ba; HFS of Ba^{137}," Physical Review, 136: A376-A379 (October 1964).

22. Bernhardt, A.F., D.E. Duerre, J.R. Simpson, and L.L. Wood. "Oscillator Strength of the Ba $6s6p\ ^1P_1$ - $6s5d\ ^1D_2$ Transition Inferred from the Photodeflection Efficiency," Journal of the Optical Society of America, 66: 416-422 (May 1976).

23. Greenlees, G.W. et al. "High Resolution Laser Spectroscopy with Minute Samples," Optics Communications, 23: 236-239 (November 1977).

24. Jessop, P.E., and F.M. Pipkin. "Measurement of the Lifetime of the $5d6p\ ^1F_3$ State of Barium," Physical Review A, 20: 269 (July 1979).

25. Benham, Vincent N. "Sodium Concentration Measurement Using Laser Induced Fluorescence," Unpublished MS thesis. School of Engineering, Air Force Institute of Technology, WPAFB, Ohio, December 1981.

26. Instruction Manual for Spectra Physics Model 375 Dye Laser with Model 376 Dye Circulator.

27. Placzek, G. "The Rayliegh and Raman Scattering," Handbuch der Radiologie, Akademische Verlagsgesellschaft VI,2: 209-374 (1934). Available as UCRL Trans No. 526(L).

28. King, David S., and P.K. Schenck. "Optogalvanic Spectroscopy," Laser Focus, 14: 50-57 (March 1978).

29. Smyth, Kermit C., and P.K. Schenck. "Optogalvanic Spectroscopy of a Neon Discharge: Mechanism Studies," Chemical Physics Letters, 55: 466-472 (May 1978).

30. Striganov, A.R., and N.S. Sventitskii. Table of Spectral Lines of Neutral and Ionized Atoms. New York, 1968.

31. Bevington, Philip R. Data Reduction and Error Analysis for the Physical Sciences. New York: McGraw-Hill, 1969.

32. Knoll, Glenn F. Radiation Detection and Measurement. New York: John Wiley & Sons,1979.

33. Marion, Jerry B. Classical Electromagnetic Radiation. New York: Academic Press, 1965.

34. Daily, John W. "Detectability Limit and Uncertainty Considerations for Laser Induced Fluorescence Spectroscopy in Flames," Applied Optics,17: 1610-1615 (May 1978).

35. George, T.V., L. Goldstein, L. Slama, and M. Yokoyama. "Molecular Scattering of Ruby-Laser Light," Physical Review, 137: A369-A380 (January 1965).

Appendix A

Correction Due to Anisotropic Fluorescence

Resonance fluorescence is not ,in general, emitted isotropically. It contains isotropic, electric dipole, electric quadrupole, and magnetic dipole radiation components (Ref 27:43-54). The anisotropy of Ba fluorescence is due primarily to the electric dipole component (Ref 23:237).

If the fluorescence is not emitted isotropically, then depending on detector location, the measured intensity may be more or less than the average over all angles. The Ba concentration can be derived directly from the measured fluorescent intensity if the intensity is isotropic. Otherwise, a correction must be introduced accounting for a measured intensity different from the average. The correction factor, derived here, is called C. In this work it is assumed that the fluorescence is a mixture of electric dipole and isotropic components, with the quadrupole and magnetic radiations neglected. C is then the ratio of powers radiated per steradian for an isotropic and mixed source. C multiplies the Ba concentration derived assuming an isotropic source.

First, the correction factor is determined for perfect dipole radiation. The power emitted per unit solid angle by a dipole is

$$\left.\frac{dP}{d\Omega}\right|_{di} = \frac{\ddot{p}^2 \sin^2\theta}{16\pi^2 c^3 \epsilon_0} \qquad (22)$$

where

p is the dipole moment, and
θ is the angle between the vertical polarization of the incident beam and the direction of the detected fluorescence (=90° in this experiment).

Therefore, the total power radiated is

$$P = \int_{4\pi} \frac{dP}{d\Omega}\, d\Omega = \frac{2\ddot{p}^2}{12\pi c^3 \epsilon_0} \quad . \tag{23}$$

If this power were emitted isotropically, then the power radiated per unit solid angle would be

$$\left.\frac{dP}{d\Omega}\right|_{iso} = \frac{2}{12} \frac{\ddot{p}^2}{c^3 \epsilon_0} \frac{1}{4\pi^2} = \frac{\ddot{p}^2}{24 c^3 \epsilon_0 \pi^2} \quad . \tag{24}$$

Therefore, the ratio of isotropic to dipole power per steradian is

$$\frac{(dP/d\Omega)_{iso}}{(dP/d\Omega)_{di}} = \frac{2}{3\sin^2\theta} \quad . \tag{25}$$

For a perfect dipole, then $C = 2/(3\sin^2\theta)$ (Ref 30:226).

By determining the extent to which the radiators behave like dipoles, a general form of C can be determined.

The relative intensities of detected power with polarizations parallel to and perpendicular to that of the incident beam are $I_{\parallel}$ and $I_{\perp}$. $I_t = I_{\parallel} + I_{\perp}$ is the total measured intensity. For isotropic radiation, $I_{\parallel} = I_{\perp}$. For a dipole source, $I_{\perp} = 0$. I_t can be written as $I_t = I_{\perp} + (I_{\perp} + \Delta I)$ since $I_{\parallel} \geq I_{\perp}$. $\Delta I = I_{\parallel} - I_{\perp}$.

For a given measurement, $I_{iso} = 2I_{\perp}$ is the intensity

behaving like isotropic radiation. $I_{di} = \Delta I$ is the intensity behaving like dipole radiation. For convenience, define $\alpha = I_\perp / I_\parallel = I_\perp / (I_\perp + \Delta I)$. For Ba , α is measured to be 0.052.

Define the ratio of isotropic to total intensity as $F_{iso} = I_{iso}/I_t$. The analogous ratio of dipole intensity to the total is $F_{di} = I_{di}/I_t$. After some algebra, these can be re-written as

$$F_{iso} = \frac{2\alpha}{(1+\alpha)} \text{ , and } F_{di} = \frac{(1-\alpha)}{(1+\alpha)} \qquad (26)$$

The fraction behaving isotropically needs no correction factor. However, the dipole fraction needs to be corrected by the $2/(3\sin^2\theta)$ term developed above.

If the Ba number density is calculated under the assumption that the resonance radiation is isotropic, the density needs to be corrected by a factor taking the form

$$C = F_{di} \cdot \frac{2}{3\sin^2\theta} + F_{iso} \cdot 1$$

$$= \frac{2}{3} \frac{1 - \alpha + 3\alpha\sin^2\theta}{(1+\alpha)\cdot\sin^2\theta}$$

$$= \frac{2}{3} \frac{1+2\alpha}{1+\alpha} \qquad \text{for } \theta = 90^\circ$$

$$= 0.70 \text{ for Ba.}$$

Appendix B

Calibration Method

This appendix is a review of the calibration method used to determine the constants $\Omega V_c \epsilon$ that appear in several equations. The method is explained more fully by Benham (Ref 24:8-10).

The vacuum cell is filled with N_2 gas to a pressure of 1 atmosphere. Then a laser beam of known power is sent through the chamber. Light that is elastically scattered (Rayliegh scattered) from the N_2 gas is directed into the detector. The power of the detected scattered signal is

$$P_R = \frac{P_\ell \, d\sigma}{A_\ell \, d\Omega} N_n \, \Omega V_c \epsilon \quad \text{(Watts)}$$

where

- P_ℓ is the laser power (W),
- A_ℓ is the beam cross sectional area seen by the detector (m^2),
- N_n is the N_2 number density (m^{-3}),
- V_c is the volume seen to scatter by the detector in (m^3),
- Ω is the solid angle subtended by the detector in (steradians),
- ϵ accounts for losses in the detection system (unitless), and
- $\frac{d\sigma}{d\Omega}$ is the differential scattering cross section for N_2 gas (m^2/steradian). (Ref 34:1116)

$\frac{d\sigma}{d\Omega}$ was measured to be 1.04×10^{-32} m^2/ster by George (Ref 35:A379).

P_R is measured with the detection system. P_ℓ, A_ℓ, and N_n are known. Therefore, $\Omega V_c \epsilon$ can be solved for and used in equation 19 for the Ba number density.

Vita

Stephen Michael Zemyan was born on 13 February 1958 in Staunton, Virginia. He lived in nearby Fort Defiance, Virginia until graduation from Fort Defiance High School in June 1976. He then attended the University of Virginia, graduating in May 1980 with the degree of Bachelor of Science in Physics. At the same time, he received his commission in the U.S. Air Force. His first assignment is to AFIT. Lt. Zemyan's permanent address is R.R. 1, Box 26, Fort Defiance, Virginia 24437.

Unclassified

SECURITY CLASSIFICATION OF THIS PAGE (When Data Entered)

REPORT DOCUMENTATION PAGE	READ INSTRUCTIONS BEFORE COMPLETING FORM
1. REPORT NUMBER: AFIT/GNE/PH/82M-13	2. GOVT ACCESSION NO.: AD-A115 534
3. RECIPIENT'S CATALOG NUMBER	
4. TITLE (and Subtitle): LASER INDUCED FLUORESCENCE OF BARIUM EVAPORATING FROM A DISPENSER CATHODE	5. TYPE OF REPORT & PERIOD COVERED: MS THESIS
	6. PERFORMING ORG. REPORT NUMBER
7. AUTHOR(s): Stephen M. Zemyan, 2nd Lt, USAF	8. CONTRACT OR GRANT NUMBER(s)
9. PERFORMING ORGANIZATION NAME AND ADDRESS: AirForce Institute of Technology (AFIT-EN) Wright-Patterson AFB, Ohio 45433	10. PROGRAM ELEMENT, PROJECT, TASK AREA & WORK UNIT NUMBERS
11. CONTROLLING OFFICE NAME AND ADDRESS: Capt. K. O'Brien, RADC/OCTP, Griffiss AFB, New York 13441	12. REPORT DATE: March 1982
	13. NUMBER OF PAGES: 69
14. MONITORING AGENCY NAME & ADDRESS (if different from Controlling Office)	15. SECURITY CLASS. (of this report): Unclassified
	15a. DECLASSIFICATION/DOWNGRADING SCHEDULE

16. DISTRIBUTION STATEMENT (of this Report)

Approved for public release; distribution unlimited

17. DISTRIBUTION STATEMENT (of the abstract entered in Block 20, if different from Report)

15 APR 1982

18. SUPPLEMENTARY NOTES

Dean for Research and Professional Development
Air Force Institute of Technology (ATC)
Wright-Patterson AFB, OH 45433

Approved for public release IAW AFR 190-17
Frederick C. Lynch, Major, USAF
Director of Public Affairs

19. KEY WORDS (Continue on reverse side if necessary and identify by block number)

Laser Induced Resonance Fluorescence
Thermionic Dispenser Cathode
Barium

20. ABSTRACT (Continue on reverse side if necessary and identify by block number)

A continuous wave dye laser is used to induce resonance fluorescence in Ba atoms evaporating from a thermionic dispenser cathode. The laser is tuned to the 553.5nm Ba I line by making use of the optogalvanic effect in a hollow cathode discharge tube. Photon counting equipment is used to measure the Ba fluorescent intensity as a function of cathode temperature and laser power. Ba concentrations and evaporation rates as functions of temperature are

DD FORM 1 JAN 73 1473 EDITION OF 1 NOV 65 IS OBSOLETE

Unclassified

SECURITY CLASSIFICATION OF THIS PAGE (When Data Entered)

derived from the fluorescent intensity.

Laser induced fluorescence is established as a technique for examining various species evaporating from cathodes. The technique can be used in attempts to determine cathode failure mechanisms.